CHEMISTRY
A European Journal

Supporting Information

Halogen-Bond Effects on the Thermo- and Photochromic Behaviour of Anil-Based Molecular Co-crystals

Andrea Carletta[+],[a] Floriana Spinelli[+],[b] Simone d'Agostino,[b] Barbara Ventura,*[c] Michele R. Chierotti,[d] Roberto Gobetto,[d] Johan Wouters,*[a] and Fabrizia Grepioni*[b]

chem_201605953_sm_miscellaneous_information.pdf

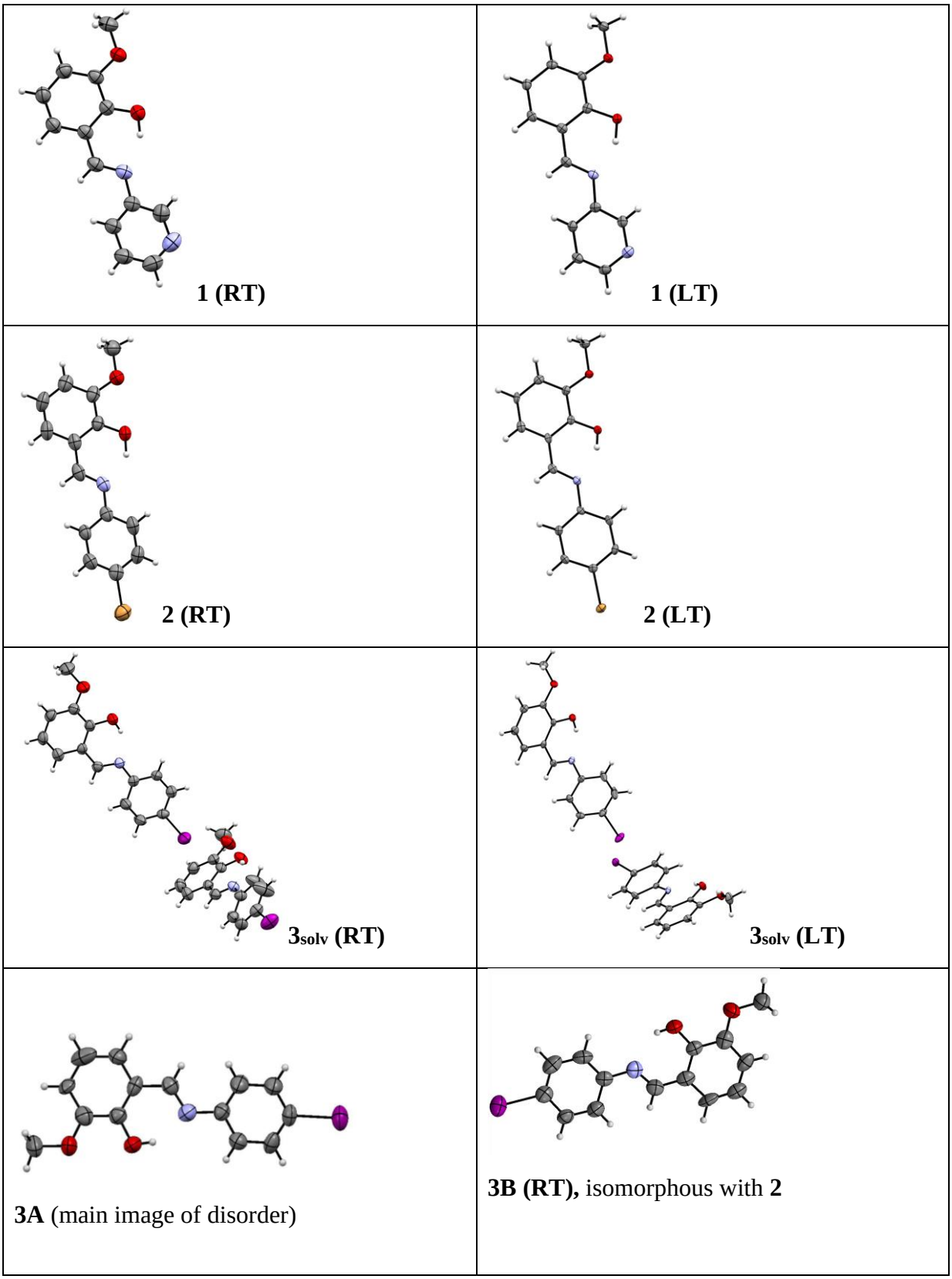

Figure S1. ORTEP diagrams for single component crystal structures.

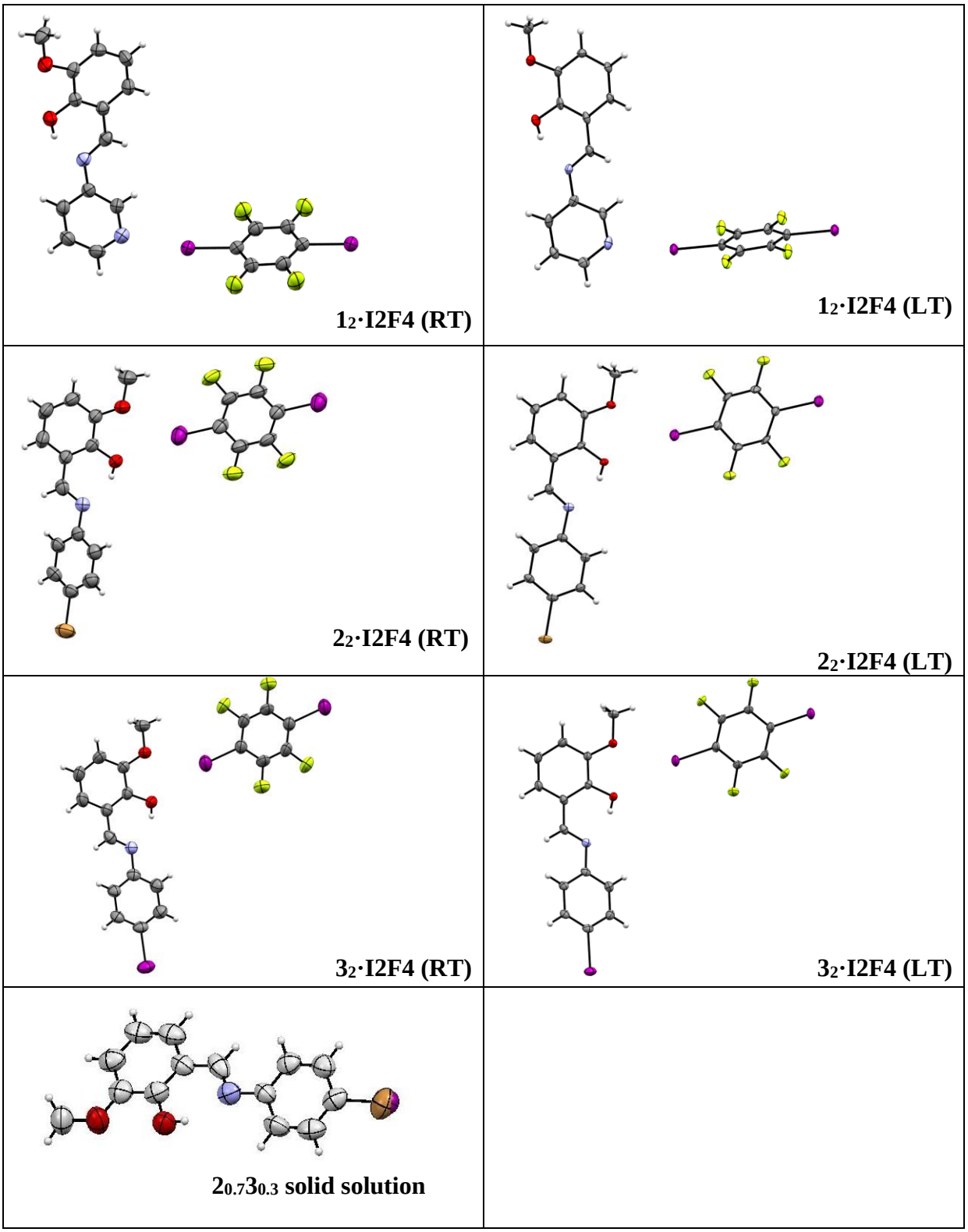

Figure S2. ORTEP diagrams for multicomponent crystal structures.

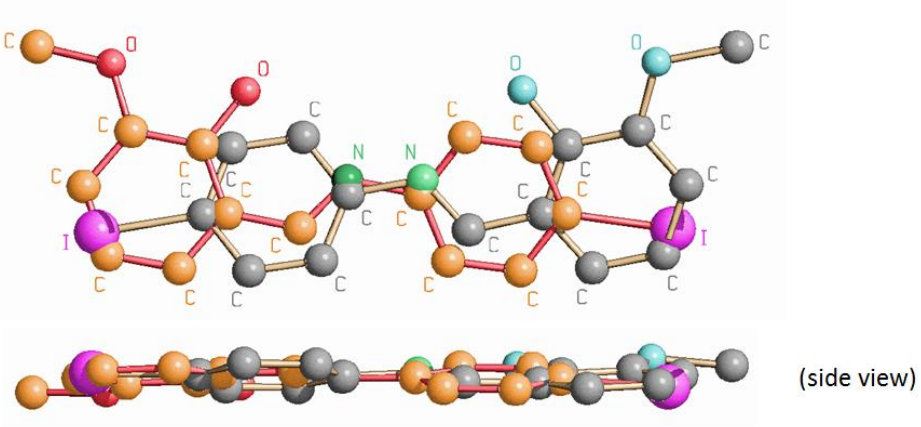

Figure S3. Disorder in 3A. The occupancy ratio is 70:30 (bonds in red define the main image)

Table S1. Crystallographic data and details of measurements for **1**, **2** and $\mathbf{3_{solv}}$ at room and low temperature.

	1 (RT)	**2 (RT)**	$\mathbf{3_{solv}}$ **(RT)**	**1 (LT)**	**2 (LT)**	$\mathbf{3_{solv}}$ **(LT)**
Empirical formula	$C_{13}H_{12}N_2O_2$	$C_{14}H_{12}BrNO_2$	$C_{14}H_{12}INO_2$	$C_{13}H_{12}N_2O_2$	$C_{14}H_{12}BrNO_2$	$C_{14}H_{12}INO_2$
Fw (g/mol)	228.25	306.16	353.15	228.25	306.16	353.15
Crystal system	Orthorhombic	Orthorhombic	Triclinic	Orthorhombic	Orthorhombic	Triclinic
Space group	$P2_12_12_1$	$P2_12_12_1$	$P\bar{1}$	$P2_12_12_1$	$P2_12_12_1$	$P\bar{1}$
a (Å)	5.6190(4)	4.9234(2)	11.2134(6)	5.5415(4)	4.8229(3)	11.0853(4)
b (Å)	9.2825(7)	12.5234(8)	12.4384(7)	9.197(3)	12.5498(11)	12.2243(6)
c (Å)	21.7490(14)	20.5990(11)	12.7482(8)	21.5766(15)	20.3554(10)	12.4559(5)
α (°)	90	90	109.977(4)	90	90	110.222(3)
β (°)	90	90	108.168(5)	90	90	106.487(4)
γ (°)	90	90	103.656(6)	90	90	102.947(5)
V (Å³)	1134.39(14)	1270.09(12)	1466.26(19)	1099.7(4)	1232.04(15)	1418.06(13)
Z	4	4	4	4	4	4
Crystal size (mm)	0.20 x 0.40 x 0.54	0.35 x 0.38 x 0.58	0.17 x 0.28 x 0.50	0.20 x 0.45 x 0.55	0.55, 0.30, 0.18	0.25 x 0.45 x 0.53
T(K)	293	293	293	108	147	108
Nref	1983	2222	5164	1783	2091	4984
Npar	160	168	329	159	168	335
R	0.0321	0.0408	0.0432	0.0347	0.0244	0.0269
GoF	1.03	1.07	1.03	1.08	1.070	1.04
wR^2	0.0791	0.0855	0.1038	0.0796	0.0479	0.0695

Table S2. Crystallographic data and details of measurements for **3A**, **3B** and $\mathbf{2_{0.7}3_{0.3}}$.

	3A	**3B**	$\mathbf{2_{0.7}\text{-}3_{0.3}}$
Empirical formula	$C_{14}H_{12}INO_2$	$C_{14}H_{12}INO_2$	$C_{14}H_{12}Br_{0.70}I_{0.30}NO_2$
Fw (g/mol)	353.16	353.15	320.25
Crystal system	Monoclinic	Orthorhombic	Orthorhombic
Space group	P21/c	P212121	P212121
a (Å)	12.3849(11)	4.958(5)	4.9488(5)
b (Å)	16.7076(10)	12.518(5)	12.5366(13)
c (Å)	6.6782(5)	21.479(5)	20.993(2)
α (°)	90	90	90
β (°)	104.83	90	90
γ (°)	90	90	90
V (Å³)	1335.78(17)	1333.1(15)	1302.5(2)
Z	4	4	4
Crystal size (mm)	0.05 x 0.04 x0.03	0.1 x 0.05 x 0.04	0.05 x 0.04 x0.03
T(K)	293	293	293
Nref	2783	2647	2968
Npar	194	166	175
R	0.0559	0.0605	0.0725
GoF	0.979	1.130	1.016
wR^2	0.1784	0.1702	0.2225

Table S3. Crystallographic data and details of measurements for **1_2·I2F4**, **2_2·I2F4** and **3_2·I2F4** at room and low temperature.

	1_2·I2F4 (RT)	**2_2·I2F4 (RT)**	**3_2·I2F4 (RT)**	**1_2·I2F4 (LT)**	**2_2·I2F4 (LT)**	**3_2·I2F4 (LT)**
Empirical formula	$C_{13}H_{12}N_2O_2$, 0.5($C_6F_4I_2$)	$C_{14}H_{12}BrNO_2$, 0.5($C_6F_4I_2$)	$C_{14}H_{12}INO_2$, 0.5($C_6F_4I_2$)	$C_{13}H_{12}N_2O_2$, 0.5($C_6F_4I_2$)	$C_{14}H_{12}BrNO_2$,0.5($C_6F_4I_2$)	$C_{14}H_{12}INO_2$, 0.5($C_6F_4I_2$)
Fw (g/mol)	429.18	507.09	554.08	429.18	507.09	554.08
Crystal system	Monoclinic	Monoclinic	Monoclinic	Monoclinic	Monoclinic	Monoclinic
Space group	$P2_1/n$	$P2_1/n$	$P2_1/n$	$P2_1/n$	$P2_1/n$	$P2_1/n$
a (Å)	4.6502(3)	7.1058(5)	7.5577(4)	4.6036(3)	7.0795(3)	7.6958(3)
b (Å)	28.0826(19)	9.4229(7)	9.2626(4)	27.982(2)	9.3289(4)	9.0189(3)
c (Å)	12.1429(8)	26.348(2)	25.9451(17)	12.0308(6)	25.9574(12)	25.5175(11)
α (°)	90	90	90	90	90	90
β (°)	94.695(6)	93.649(8)	96.577(5)	96.165(5)	93.004(4)	98.428(4)
γ (°)	90	90	90	90	90	90
V (Å³)	1580.42(18)	1760.6(2)	1804.31(17)	1540.82(17)	1711.97(13)	1751.98(12)
Z	4	4	4	4	4	4
Crystal size (mm)	0.10 x 0.20 x 0.35	0.15 x 0.29 x 0.56	0.17 x 0.50 x 0.60	0.05 x 0.25 x 0.60	0.20 x 0.34 x 0.60	0.28 x 0.37 x 0.60
T(K)	293	293	293	115	105	150
Nref	2795	3102	3159	2724	3014	3001
Npar	210	223	222	213	222	222
R	0.0409	0.0411	0.0374	0.0574	0.0281	0.0211
GoF	1.11	1.08	1.09	1.12	1.00	1.30
wR^2	0.0805	0.0978	0.0869	0.1451	0.0616	0.0527

Table S4. Selected parameters for halogen bonds.

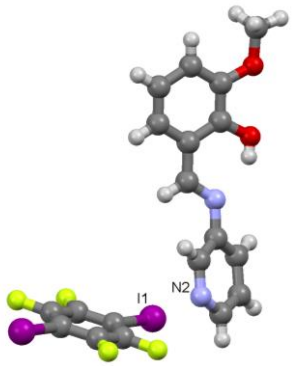	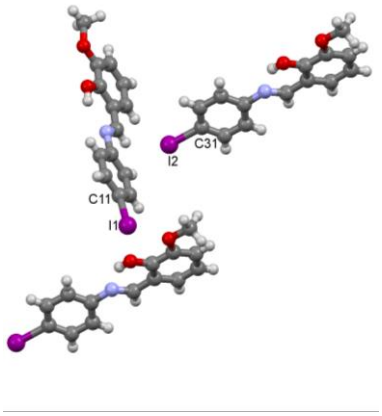	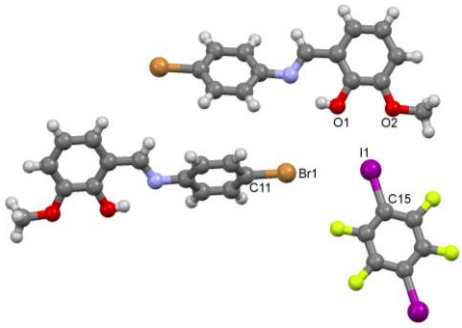
1_2·I2F4	**3_{solv}**	**2_2·I2F4**

	halogen…halogen interaction (type II)				Halogen bond		
	Contact type	**X…X distance (Å)**	**θ1 (deg) (C11-X…I)**	**θ2 (deg) (X…I –C15)**	**Contact type**	**A…I distance (Å) (A = O, N)**	**A…I–C angle (deg) (A = O, N)**
1_2·I2F4	/	/	/	/	I1...N2	2.878(4)	168.9
1_2·I2F4 (LT)	/	/	/	/	I1...N2	2.855(6)	168.5
2_2·I2F4	I1...Br1	3.9239(9)	173.4	106.5	I1...O1 I1...O2	3.447(4) 3.263(4)	169.1 141.3
2_2·I2F4 (LT)	I1...Br1	3.8775(6)	173.8	107.5	I1...O1 I1...O2	3.442(2) 3.208(2)	169.0 141.6
3_2·I2F4	I2...I1	3.9568(7)	173.5	108.4	I2...O1 I2...O2	3.501(3) 3.243(3)	169.3 145.1
3_2·I2F4 (LT)	I2...I1	3.8810(5)	172.3	107.8	I2...O1 I2...O2	3.488(2) 3.198(2)	168.8 145.5
	C–I…π halogen bond						
	Contact type	**I…Cg distance (Å)**		**C…Cg distance (Å)**		**C–I…Cg angle (deg)**	
3_{solv}	C31–I2…Cg1	3.56		5.66		178.7	
	C11–I1…Cg2	3.57		5.63		166.5	
3_{solv} (LT)	C31–I2…Cg1	3.46		5.56		177.7	
	C11–I1…Cg2	3.46		5.52		160.3	
Cg1 = calculated at C8-C13 six-membered ring (molecule A) Cg2 = calculated at C21-C27 bond (molecule A)							

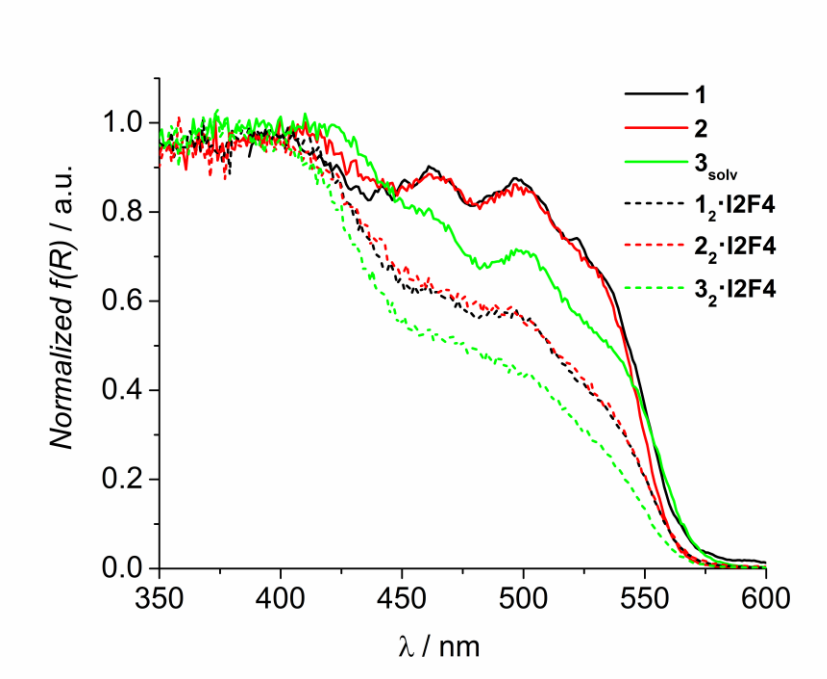

Figure S4. Normalized absorption spectra of single crystal samples of compounds **1**, **2**, **3**$_{solv}$ and respective co-crystals.

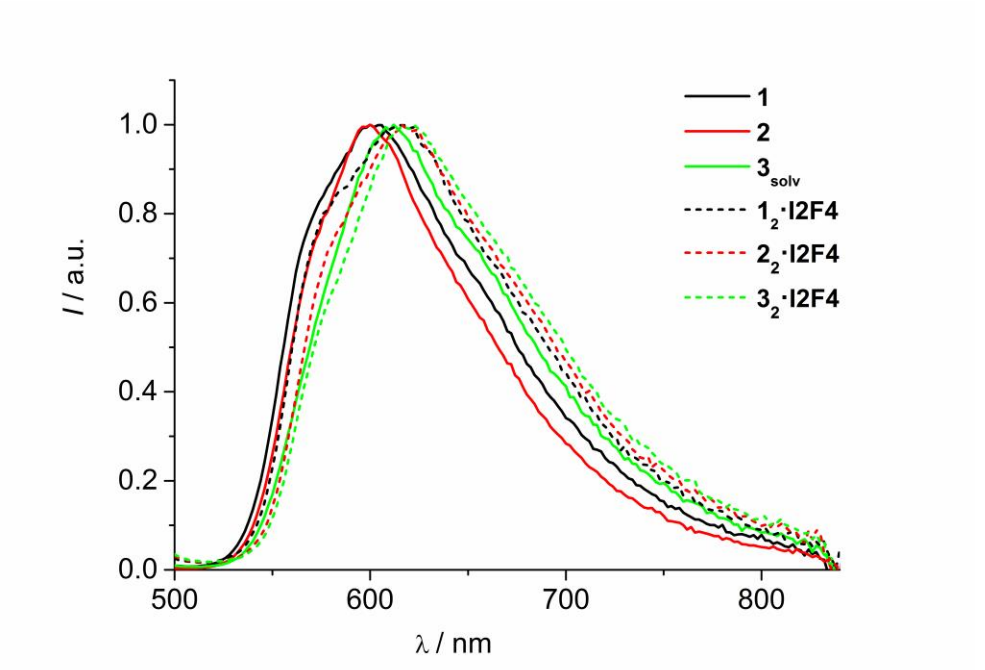

Figure S5. Normalized room temperature emission spectra of single crystal samples of compounds **1**, **2**, **3**$_{solv}$ and respective co-crystals. λ_{exc} = 480 nm.

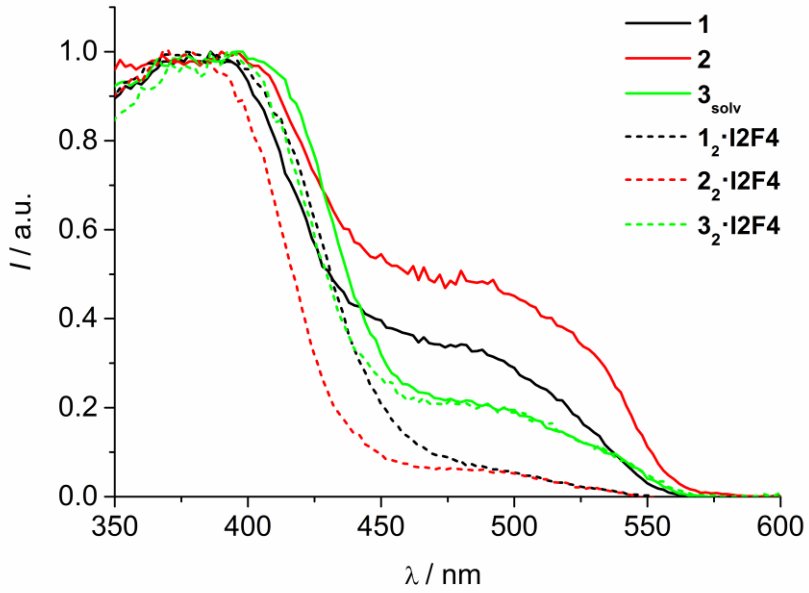

Figure S6. Normalized room temperature excitation spectra of powder samples of compounds **1**, **2**, **3$_{solv}$** and respective co-crystals. λ_{em} = 650 nm.

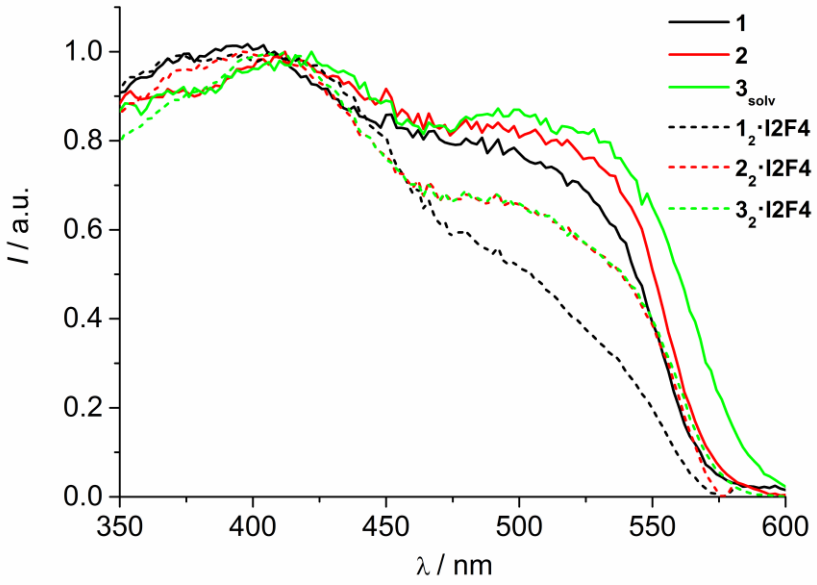

Figure S7. Normalized room temperature excitation spectra of single crystal samples of compounds **1**, **2**, **3$_{solv}$** and respective co-crystals. λ_{em} = 660 nm.

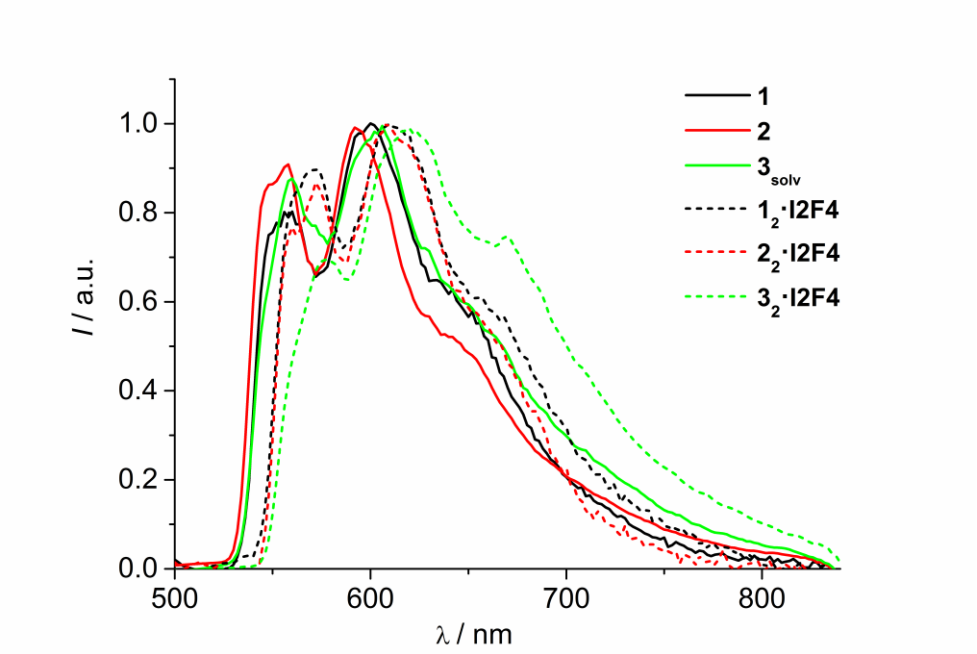

Figure S8. Normalized emission spectra at 77 K of single crystal samples of compounds **1**, **2**, **3**$_{solv}$ and respective co-crystals. λ_{exc} = 450 nm.

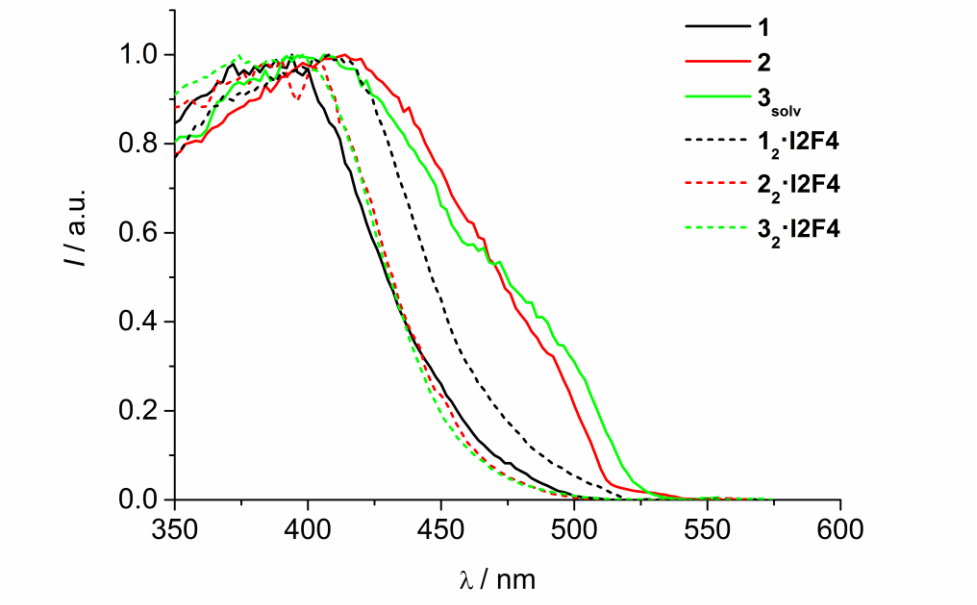

Figure S9. Normalized excitation spectra at 77 K of powder samples of compounds **1**, **2**, **3**$_{solv}$ and respective co-crystals. λ_{em} = 600/620 nm.

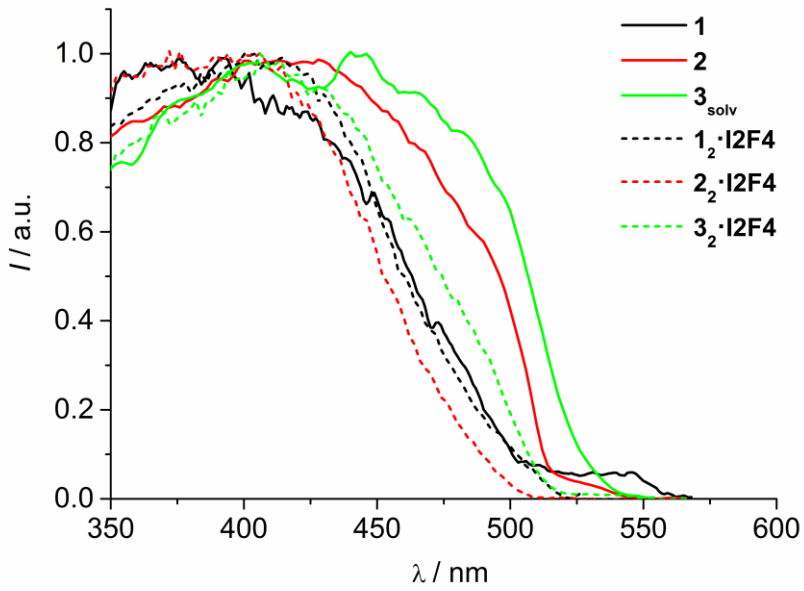

Figure S10. Normalized excitation spectra at 77 K of single crystal samples of compounds **1**, **2**, **3**$_{solv}$ and respective co-crystals. λ_{em} = 600 nm.

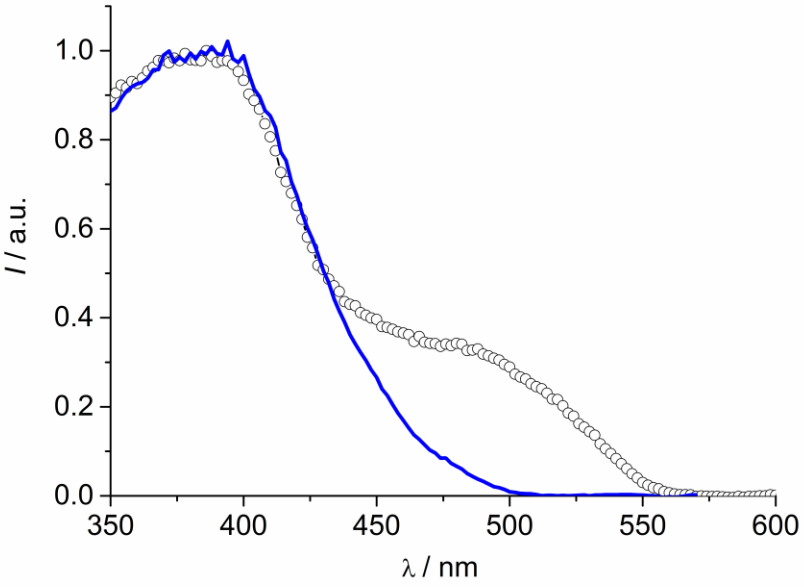

Figure S11. Normalized excitation spectra of compound **1** (powder sample) at room temperature (open dots, λ_{em} = 650 nm) and at 77 K (blue line, λ_{em} = 600 nm).

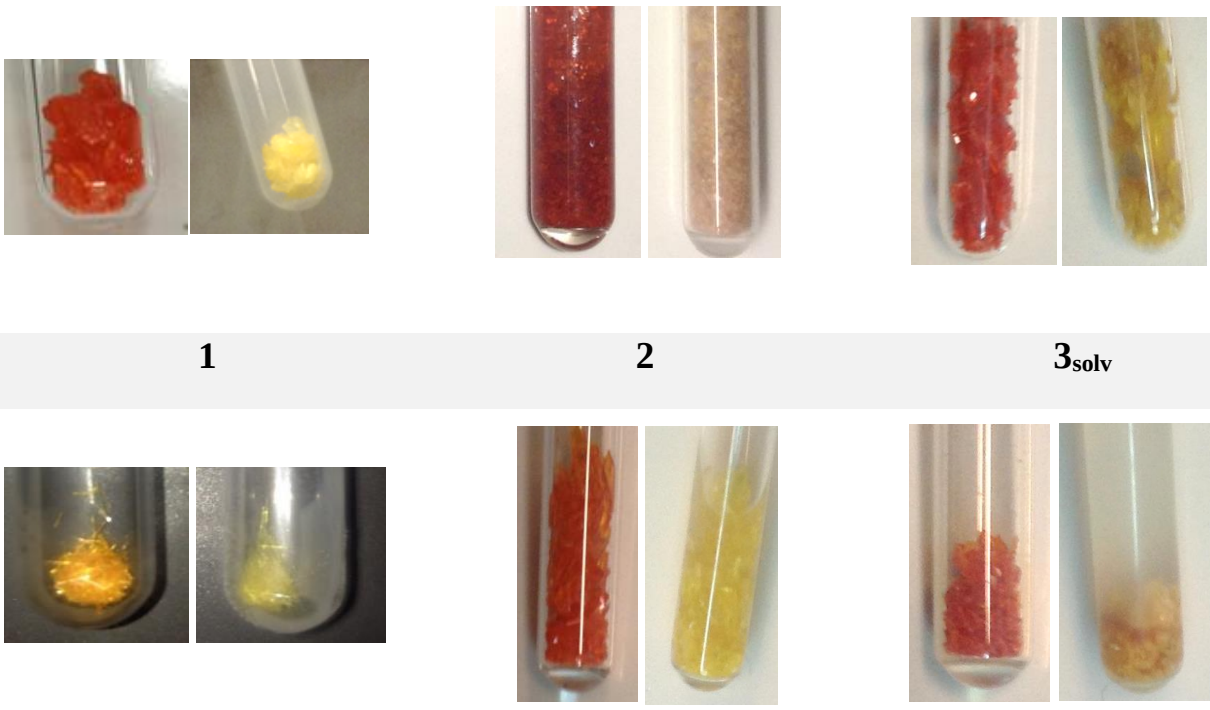

Figure S12. Thermochromism in **1**, **2**, $\mathbf{3_{solv}}$ and respective co-crystals before (left) and after (right) immersion in liquid nitrogen (77 K).

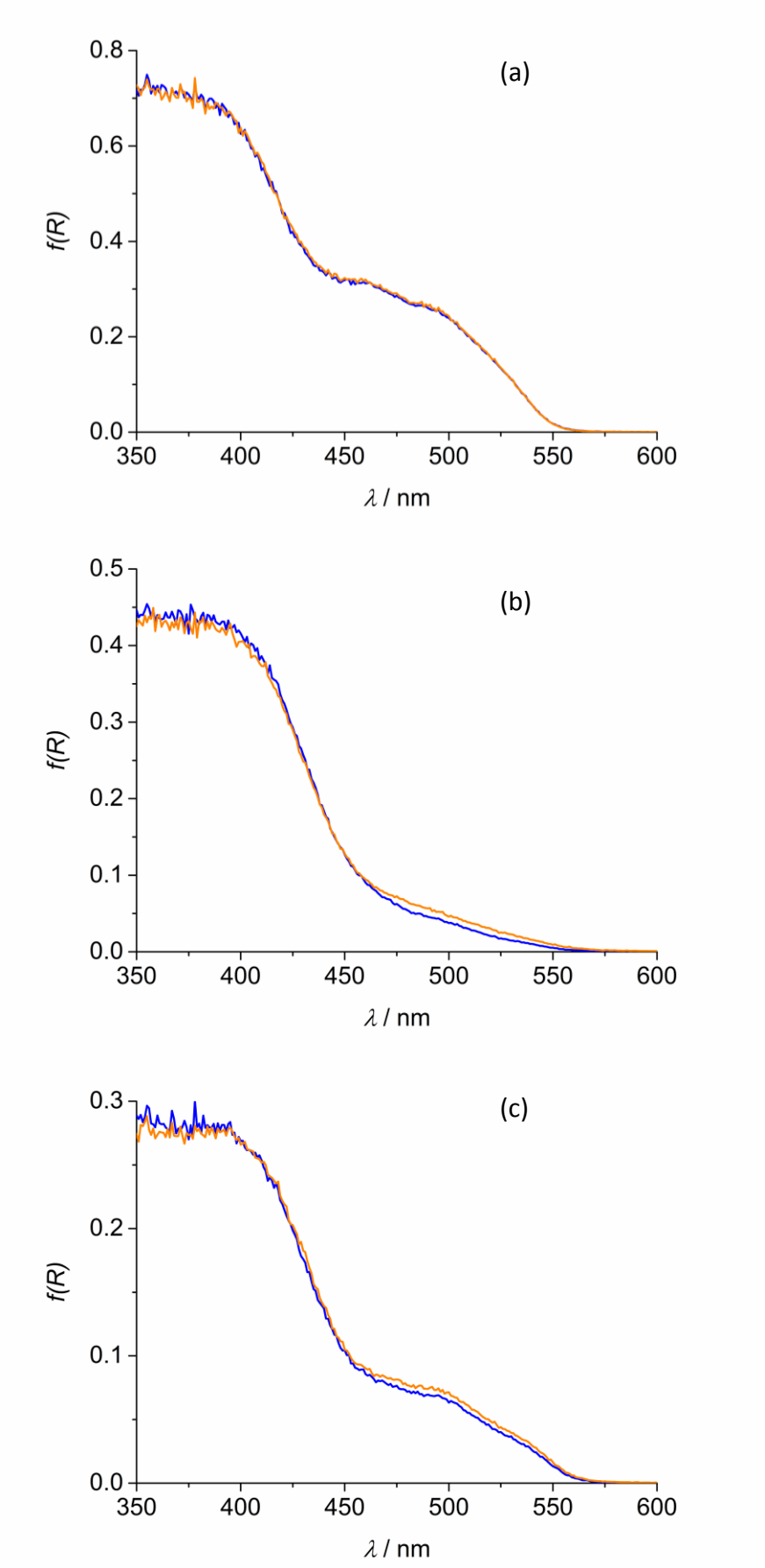

Figure S13. Absorption spectra of powder samples of compounds **1** (a), **1_2·I2F4** (b), and **3_{solv}** (c) before (blue) and after (orange) HP irradiation (see Experimental Section for details) at 365 nm for 20 min.

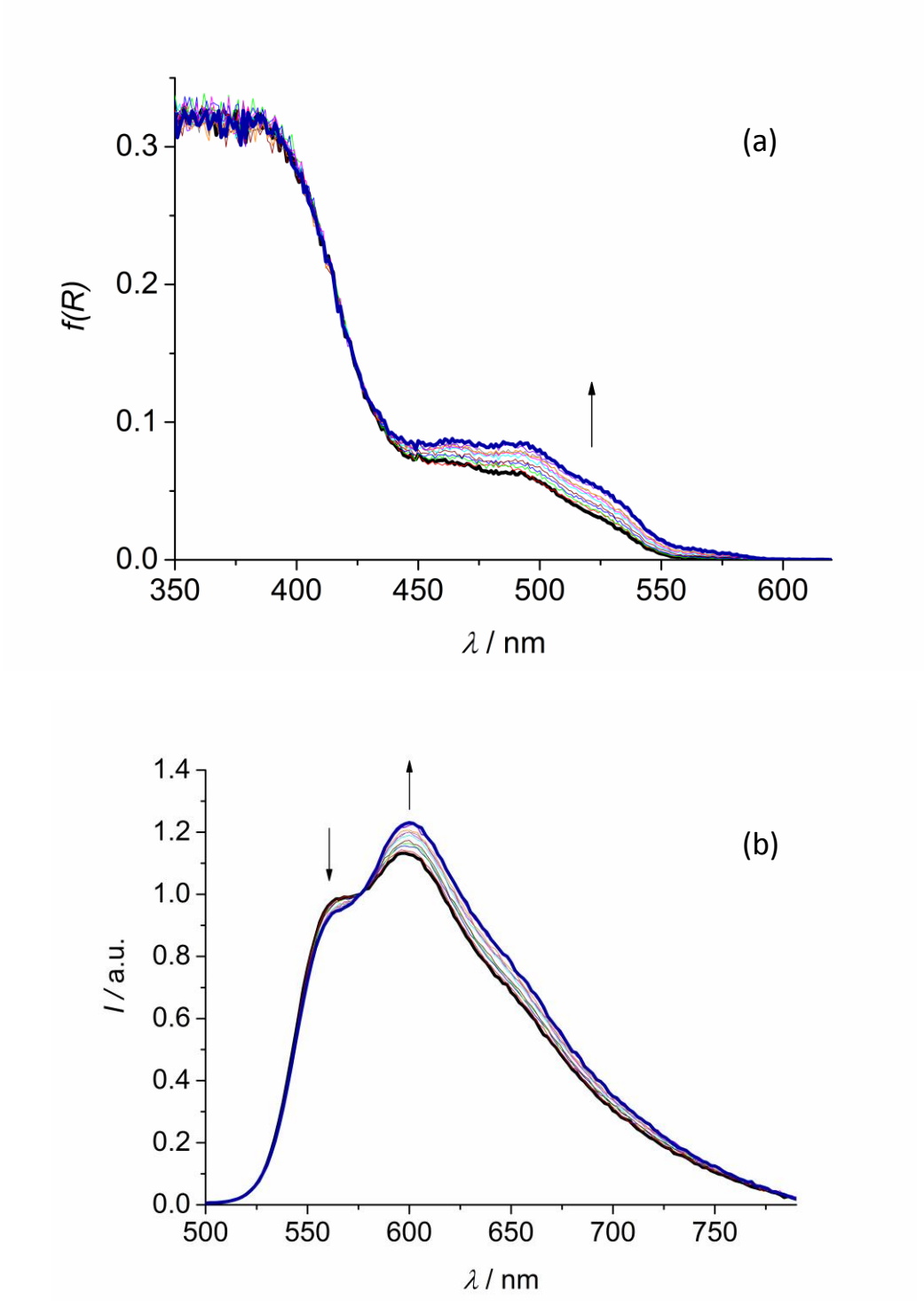

Figure S14. Absorption (a) and emission (b) spectra of **2** before (black thick) and after (blue thick) irradiation at 365 nm for 40 min (20 min LP and 20 min HP, see Experimental Section for details). Thin lines represent spectra at intermediate times. In (b) the spectra are arbitrarily normalized at 576 nm; λ_{exc} = 400 nm.

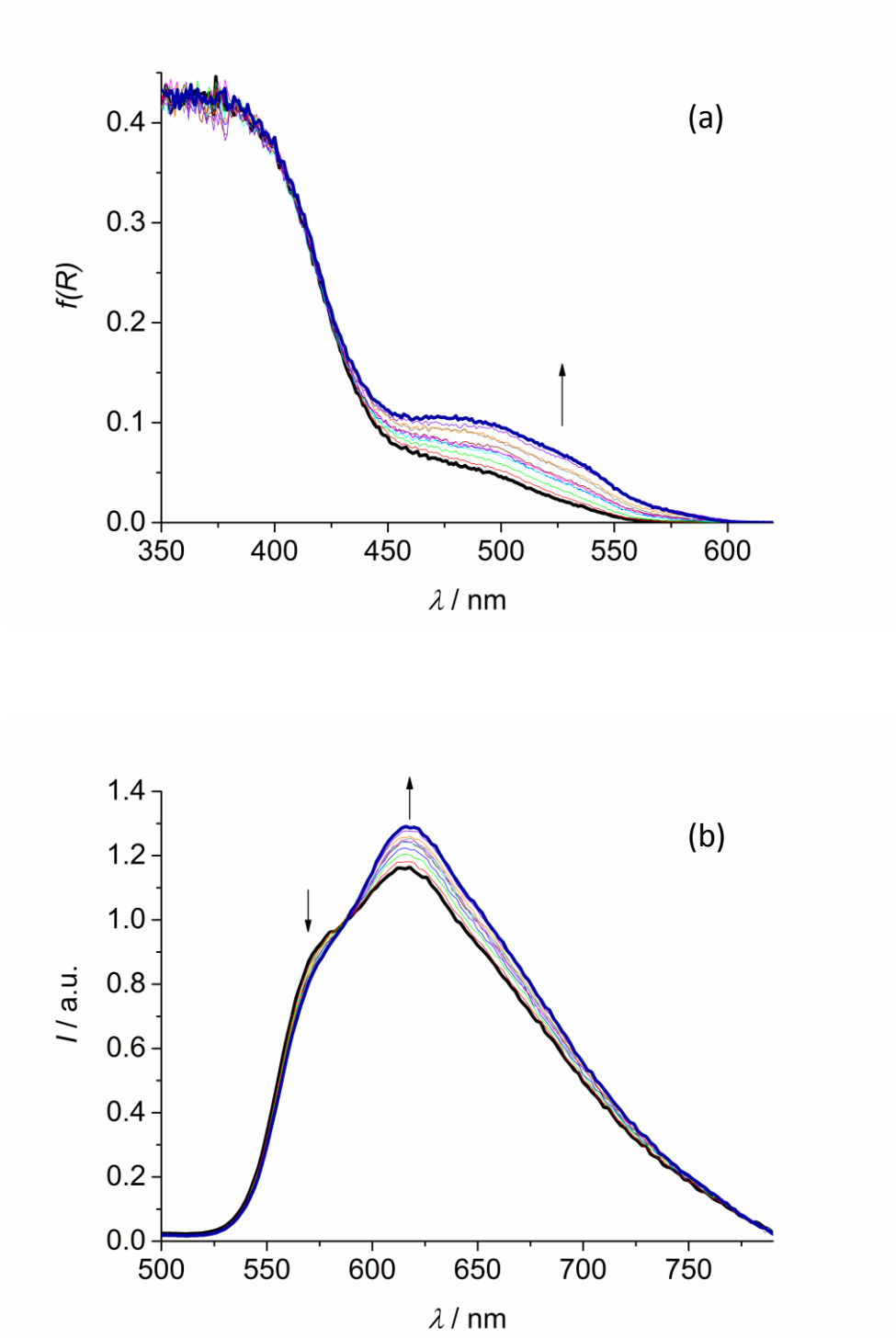

Figure S15. Absorption (a) and emission (b) spectra of **2_2·I2F4** before (black thick) and after (blue thick) irradiation at 365 nm for 40 min (20 min LP and 20 min HP, see Experimental Section for details). Thin lines represent spectra at intermediate times. In (b) the spectra are arbitrarily normalized at 588 nm; λ_{exc} = 400 nm.

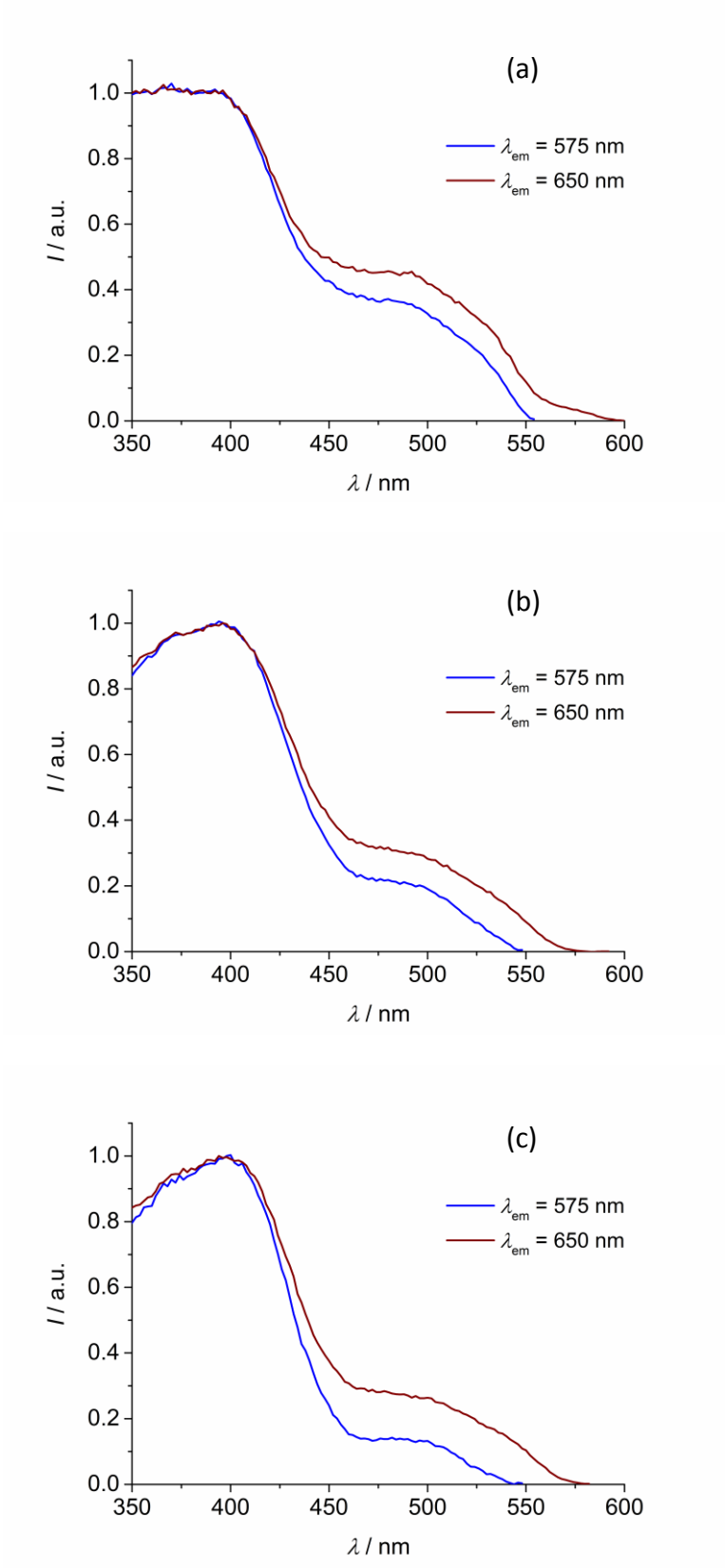

Figure S16. Normalized excitation spectra of powder samples of **2** (a), **2**$_2$**·I2F4** (b) and **3**$_2$**·I2F4** (c) collected at 575 nm and 650 nm in the photostationary state.

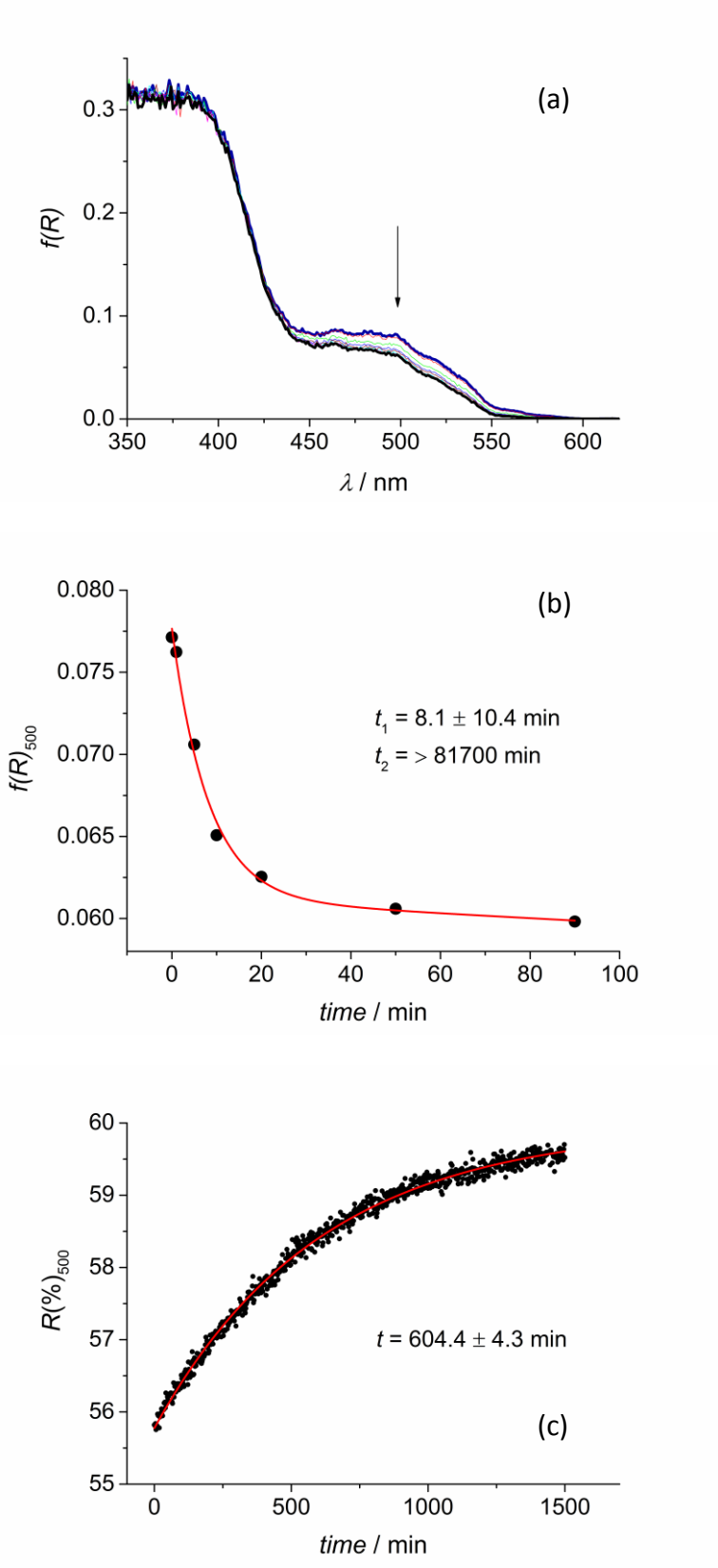

Figure S17. (a) Absorption spectral changes of **2** starting from the photostationary state and following irradiation at 465 nm for 90 min. (b) Data points at 500 nm from graph (a) and bi-exponential fitting (red). (c) Variation of the reflectance of **2** at 500 nm as a function of time, starting from the photostationary state and following the thermal back reaction; in red the mono-exponential fitting.

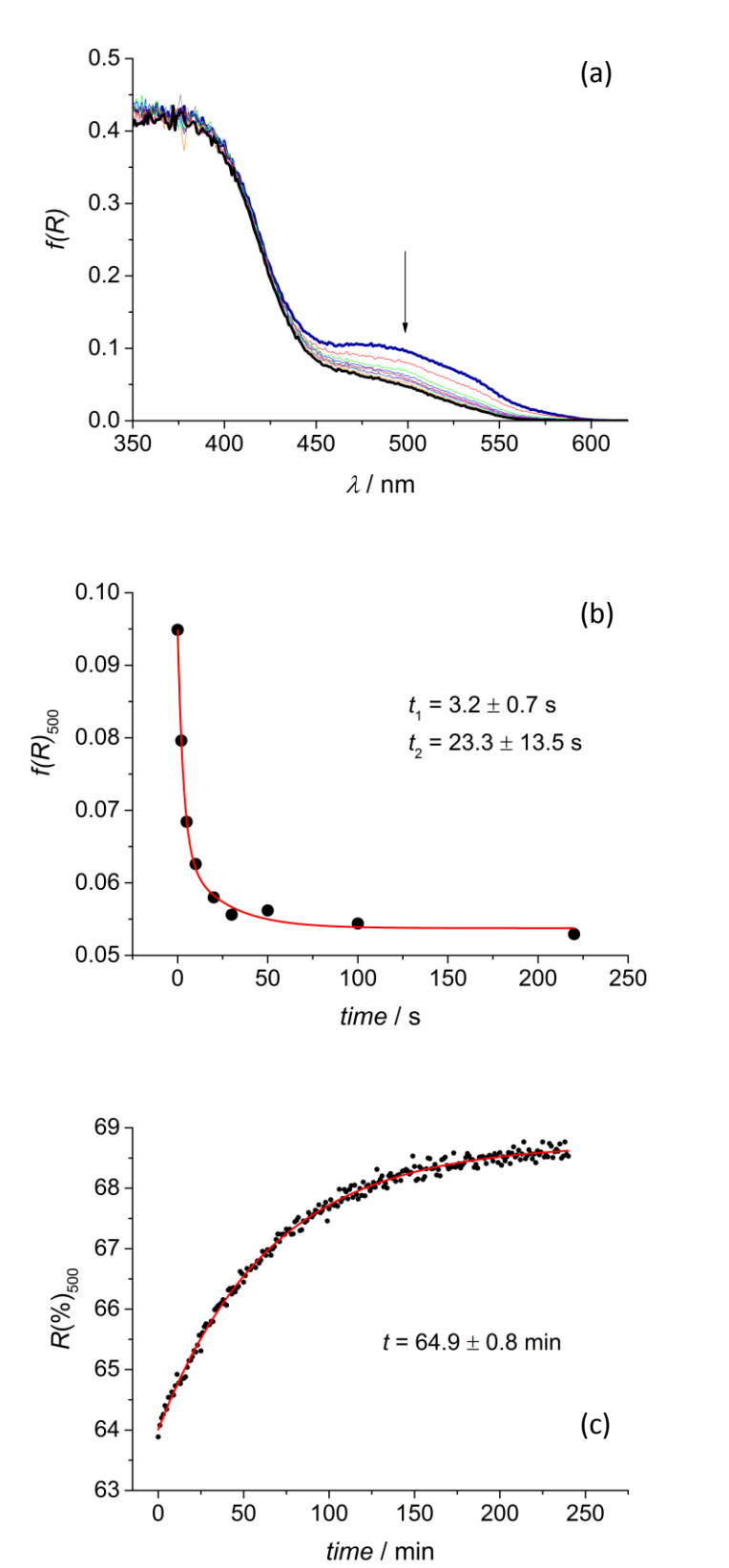

Figure S18. (a) Absorption spectral changes of **2_2·I2F4** starting from the photostationary state and following irradiation at 465 nm for 220 s. (b) Data points at 500 nm from graph (a) and bi-exponential fitting (red). (c) Variation of the reflectance of **2_2·I2F4** at 500 nm as a function of time, starting from the photostationary state and following the thermal back reaction; in red the mono-exponential fitting.

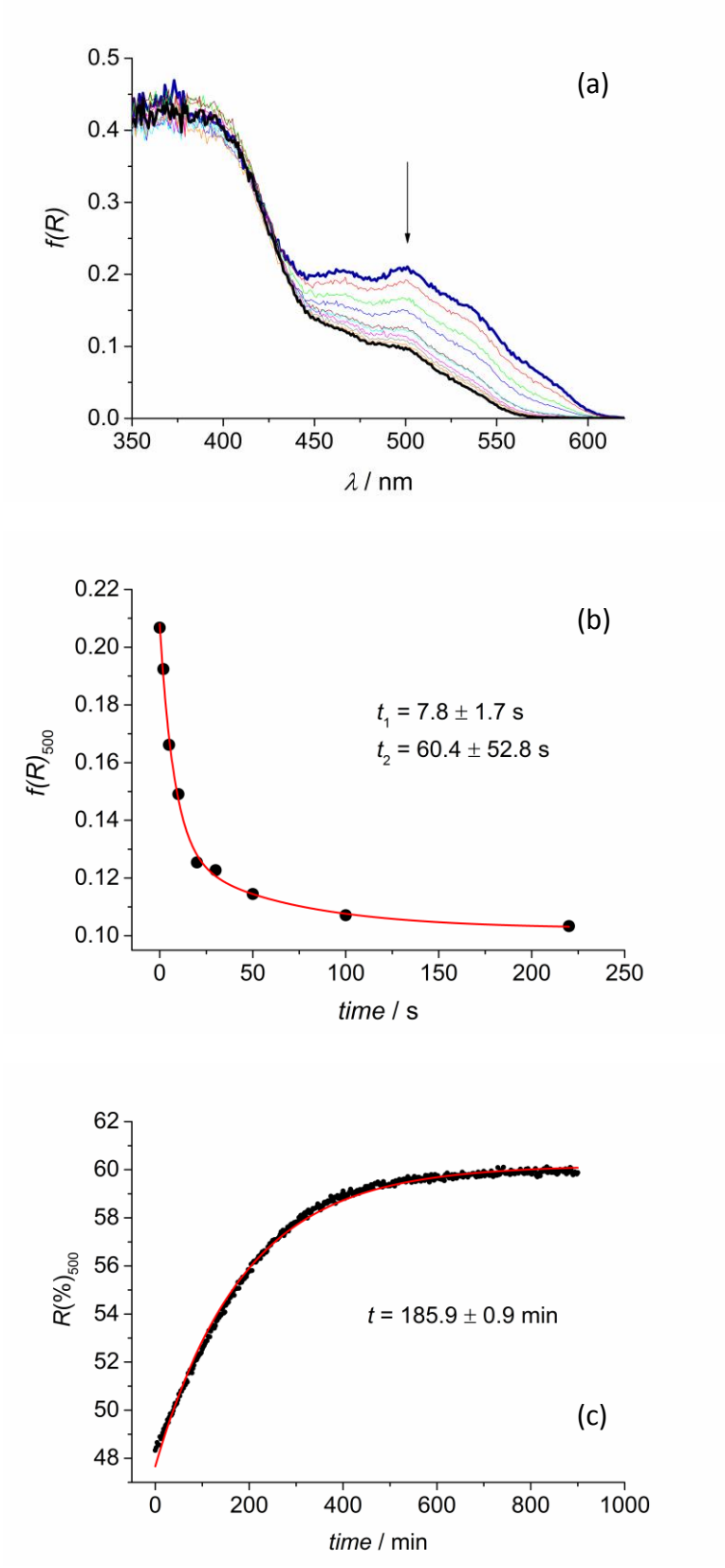

Figure S19. (a) Absorption spectral changes of **3_2·I2F4** starting from the photostationary state and following irradiation at 465 nm for 220 s. (b) Data points at 500 nm from graph (a) and bi-exponential fitting (red). (c) Variation of the reflectance of **3_2·I2F4** at 500 nm as a function of time, starting from the photostationary state and following the thermal back reaction; in red the mono-exponential fitting.

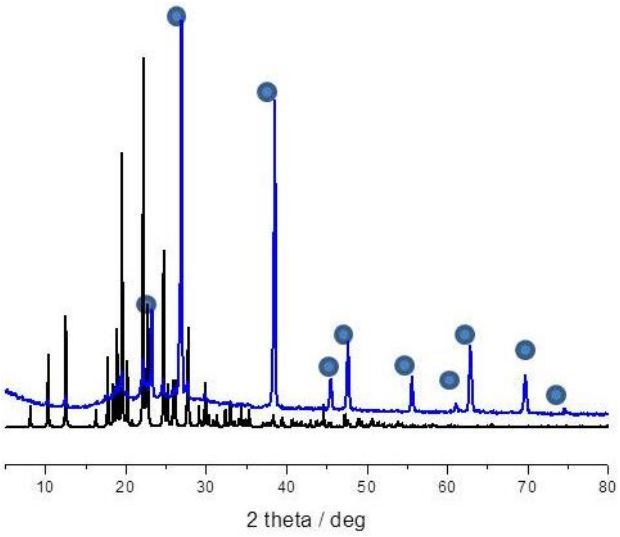

(a)

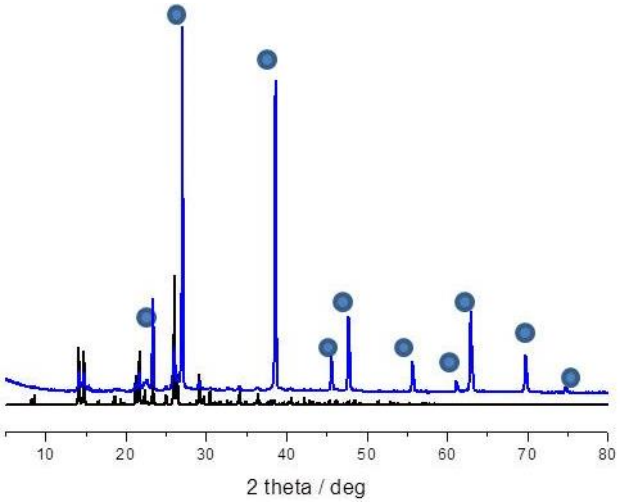

(b)

Figure S20. Powder X-ray diffraction patterns recorded on crushed KBr pellets containing samples of **1** (a) and **2** (b). Experimental (blue line) and simulated (black line) X-ray powder diffraction patterns. Blue circles indicate the KBr phase.

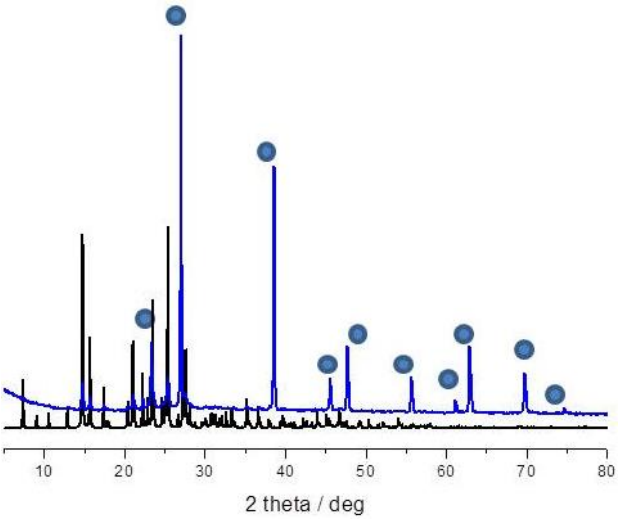

(a)

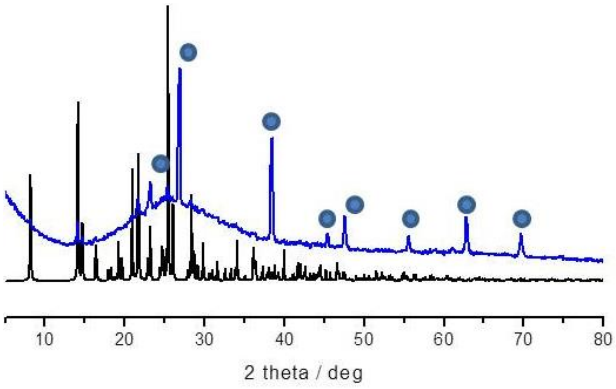

(b)

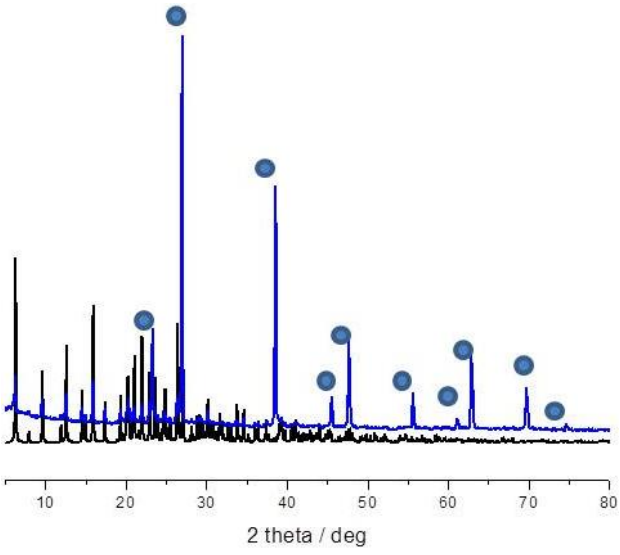

(c)

Figure S21. Powder X-ray diffraction patterns recorded on crushed KBr pellets containing samples of **3a** (a), **3** (b) and **1_2·I2F4** (c). Experimental (blue line) and simulated (black line) X-ray powder diffraction patterns. Blue circles indicate the KBr phase.

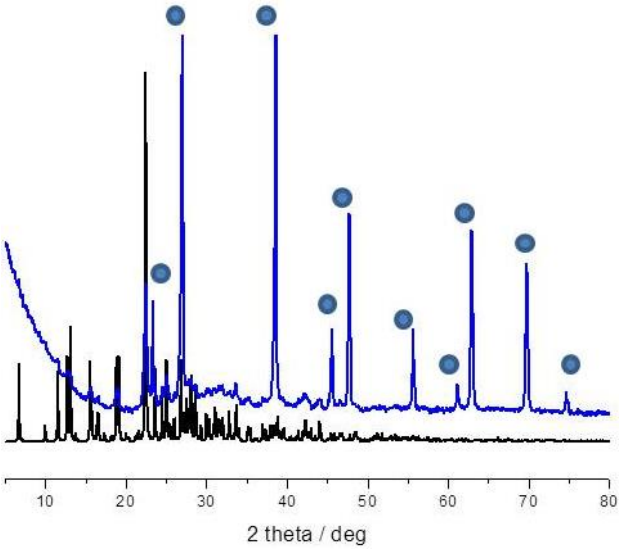

(a)

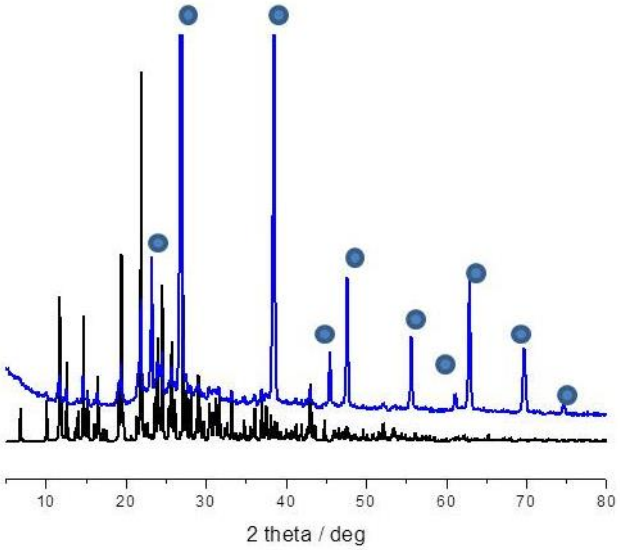

(b)

Figure S22. Powder X-ray diffraction patterns recorded on crushed KBr pellets containing samples of **2_2·I2F4** (a) and **3_2·I2F4** (b). Experimental (blue line) and simulated (black line) X-ray powder diffraction patterns. Blue circles indicate the KBr phase.

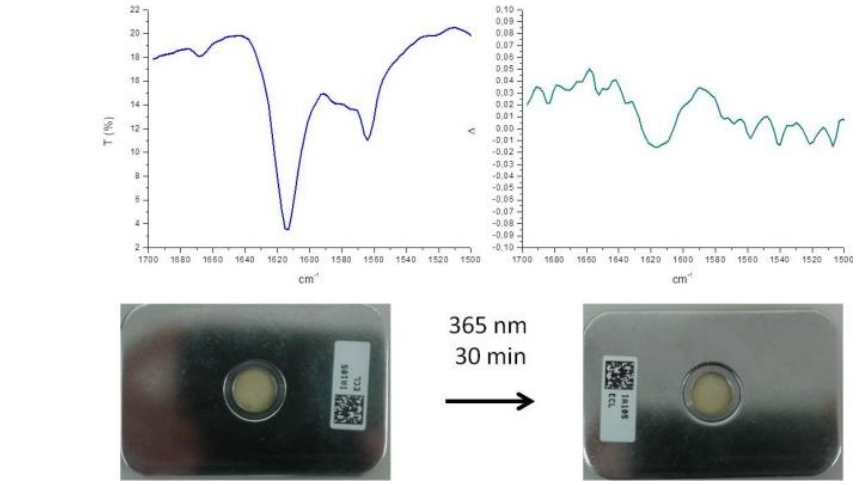

(a)

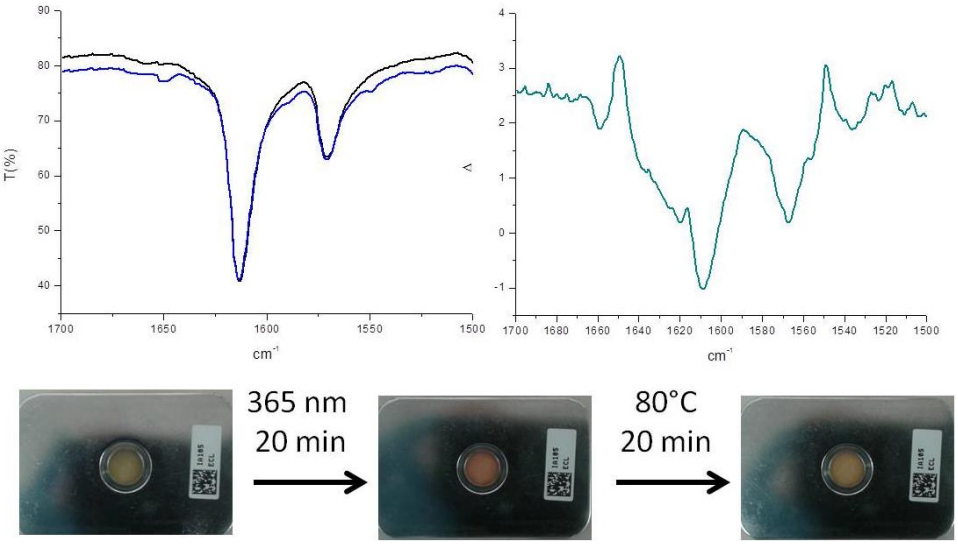

(b)

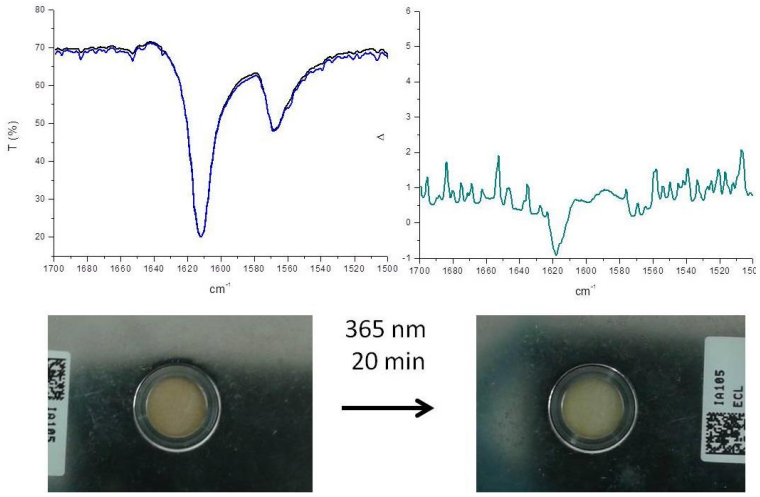

(c)

Figure S23. FTIR spectra and pictures for compounds **1** (a), **2** (b) and **3a** (c) dispersed in KBr pellets.

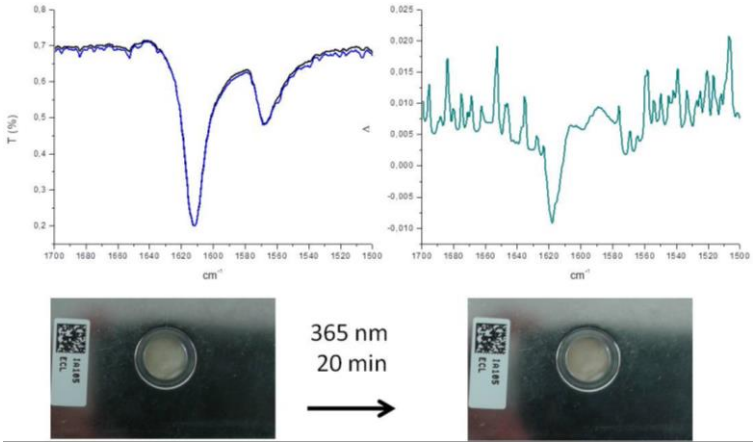

(d)

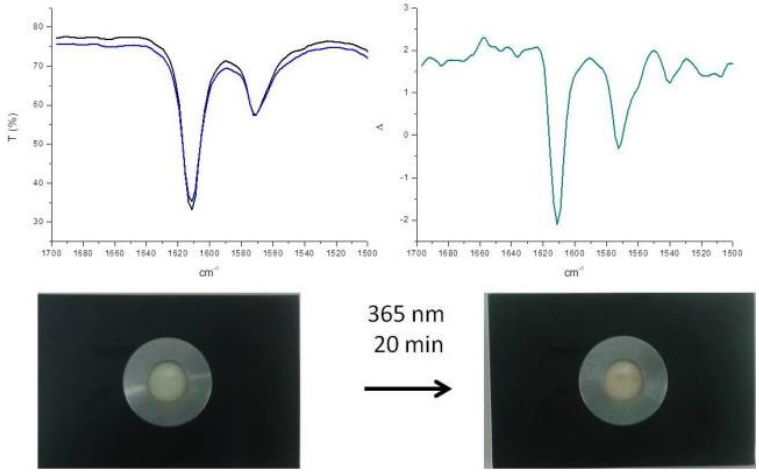

(e)

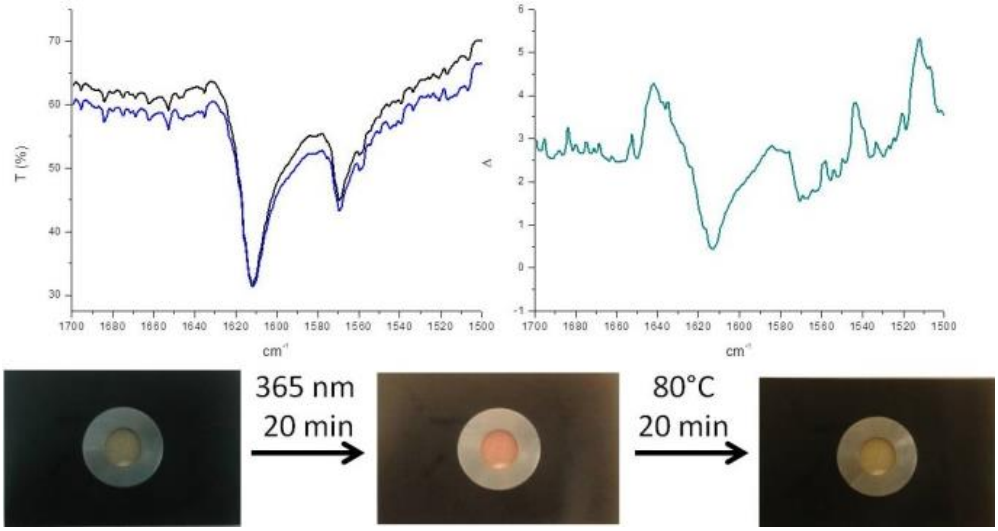

(f)

Figure S24. FTIR spectra and pictures for compounds **3b** (a), and co-crystals **1_2·I2F4** (b) and **3_2·I2F4** (c) dispersed in KBr pellets.

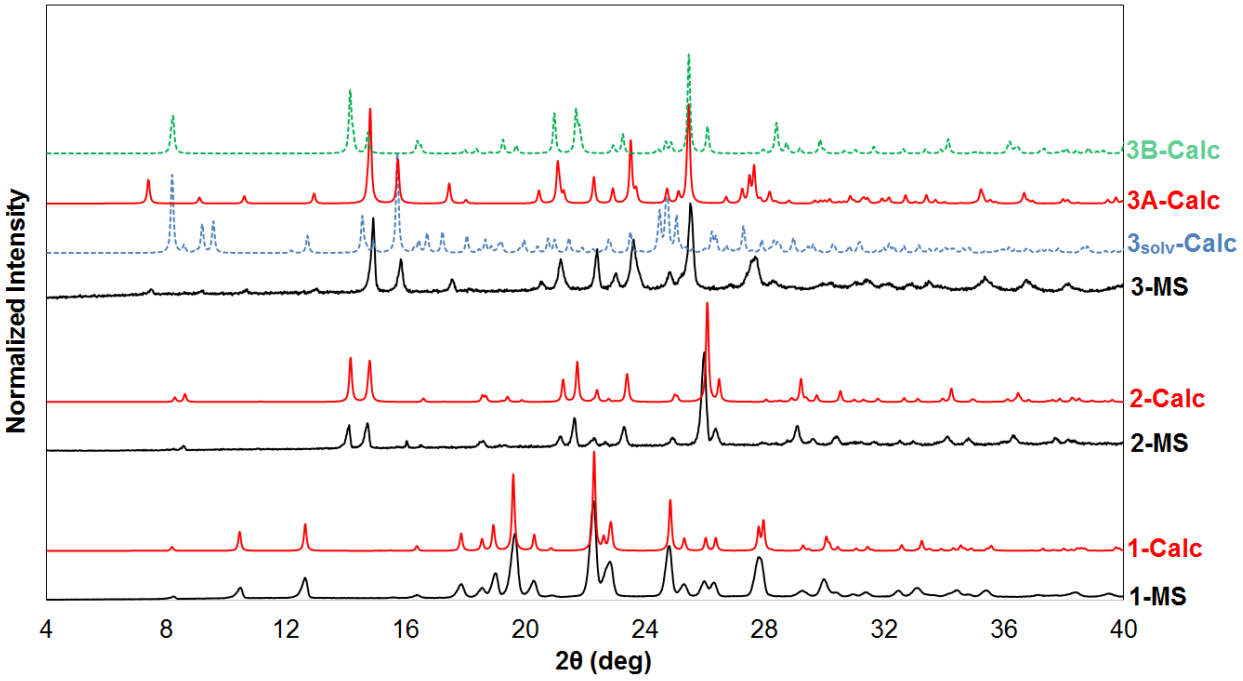

MS = mechanosynthesis Calc = calculated

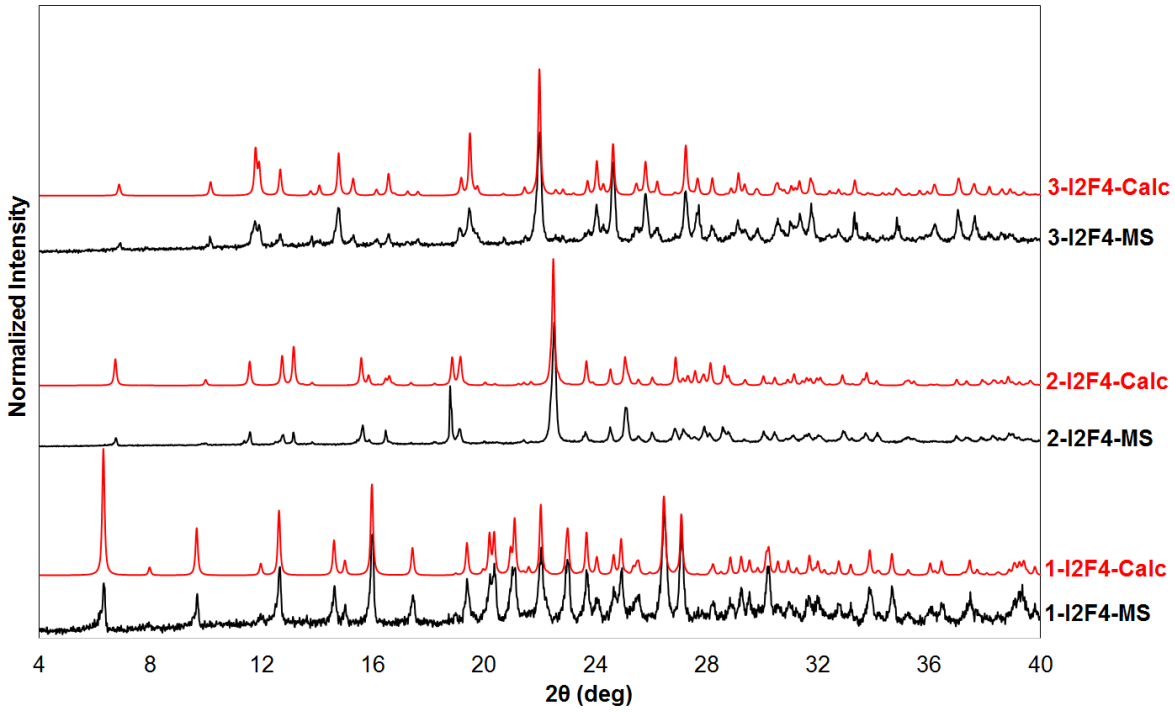

Figure S25. PXRD of the as mechanosynthesized powder products. Syntheses of the starting compounds (top) and of their cocrystals (bottom).

Table S5. Solid-state NMR acquisition parameters for samples **1**, **2** and **3$_{solv}$** and their co-crystals.

	^{13}C		^{15}N		
sample	**Resolution (Hz)**	**scans**	**Resolution (Hz)**	**scans**	**Relaxation delay (s)**
1	30	274	30	8000	11.4
1$_2$·I2F4	30	1700	30	11000	14.8
2	30	2500	26	10500	6.0
2$_2$·I2F4	30	1000	26	34000	7.3
3	30	1600	31	27500	9.1
3$_2$·I2F4	30	8000	26	14000	5.8

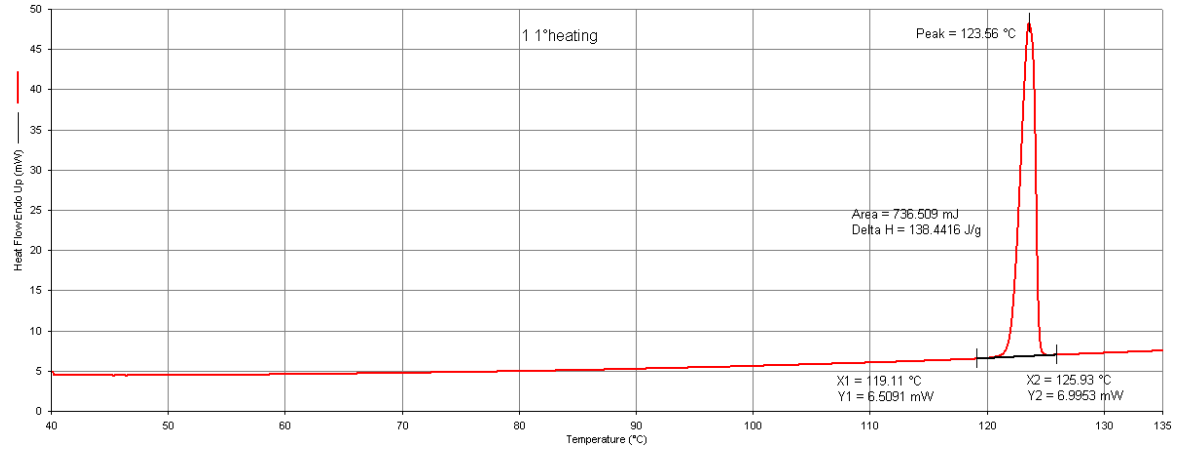

Figure S26 Thermogram of the compound **1.**

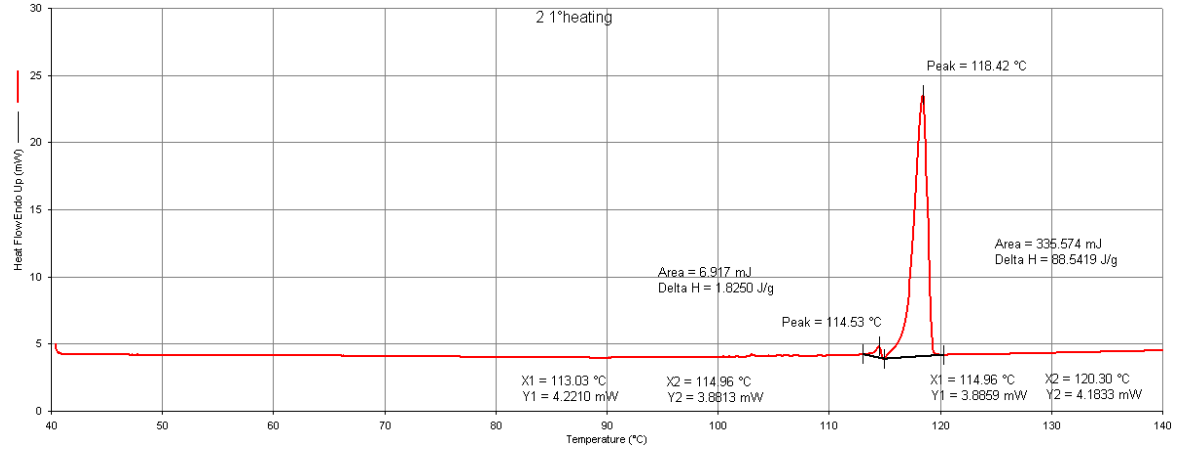

Figure S27 Thermogram of the compound **2.**

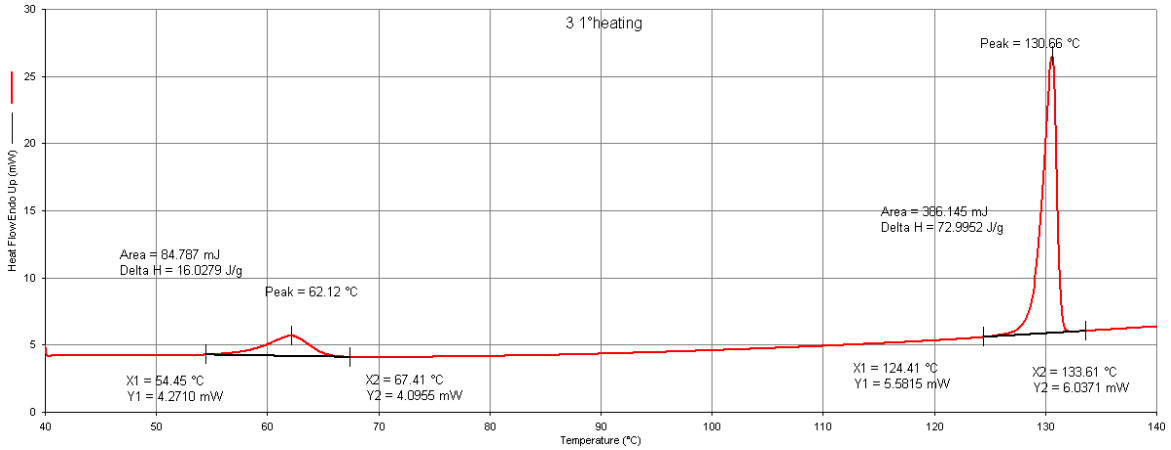

Figure S28 Thermogram of the compound **3.**

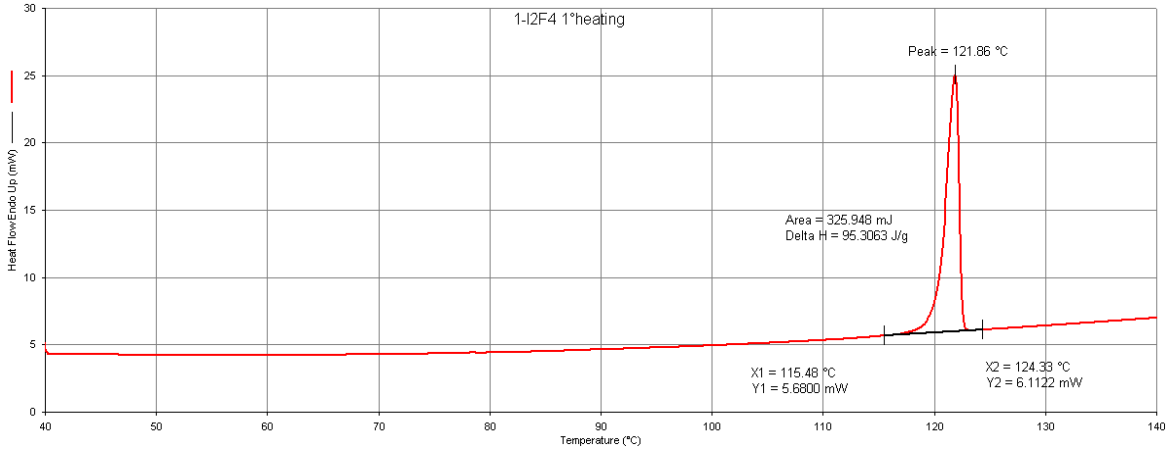

Figure S29 Thermogram of the compound **1_2·I2F4.**

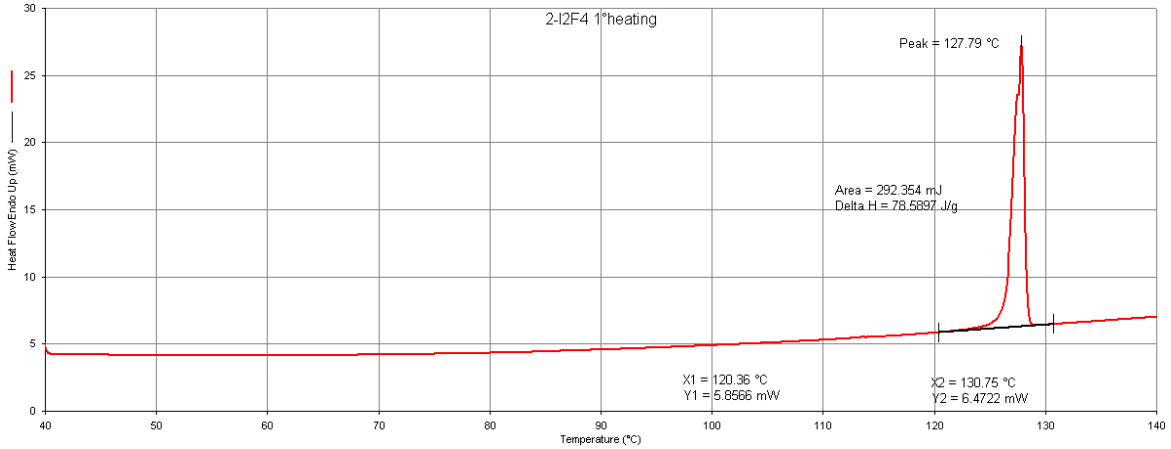

Figure S30 Thermogram of the compound **2_2·I2F4.**

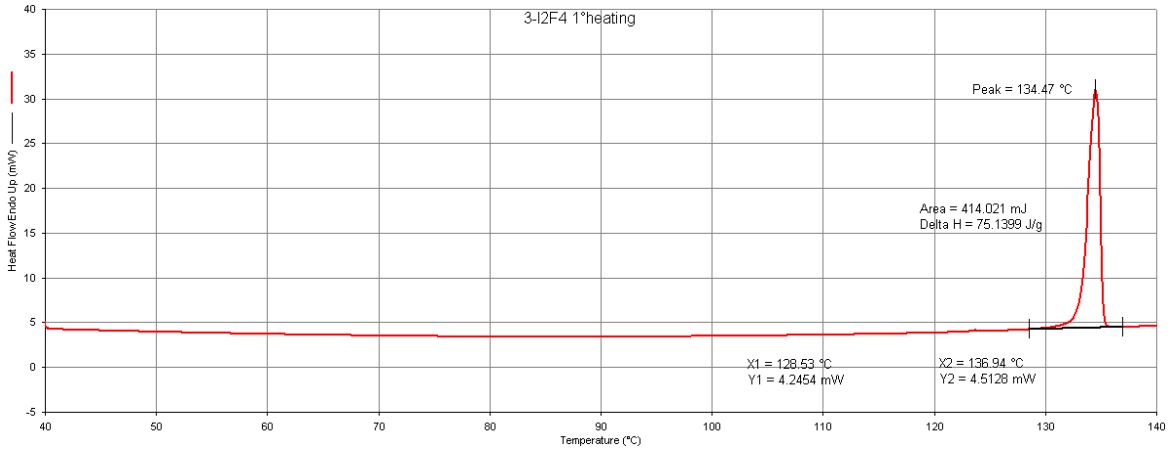

Figure S31 Thermogram of the compound **3_2·I2F4.**

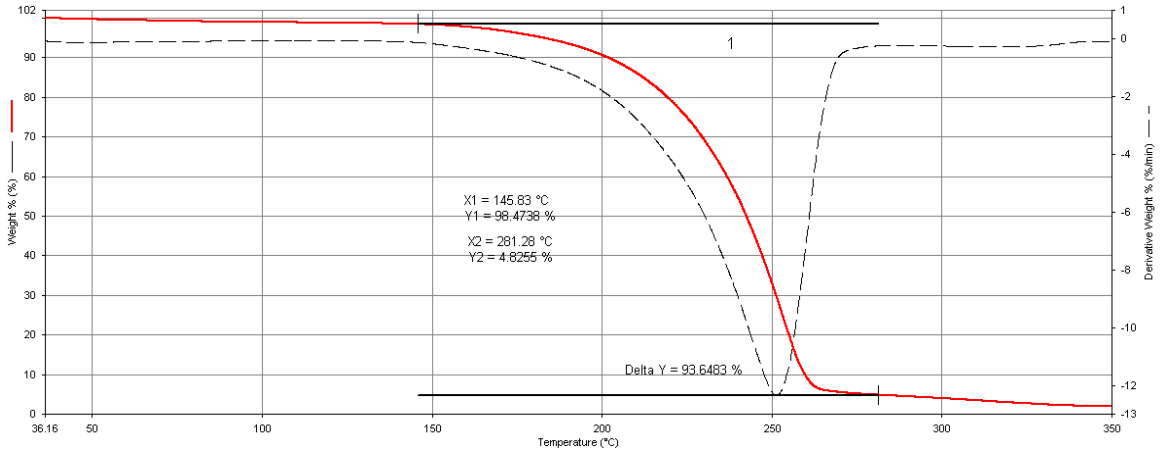

Figure S32 DSC measurement of the compound **1.**

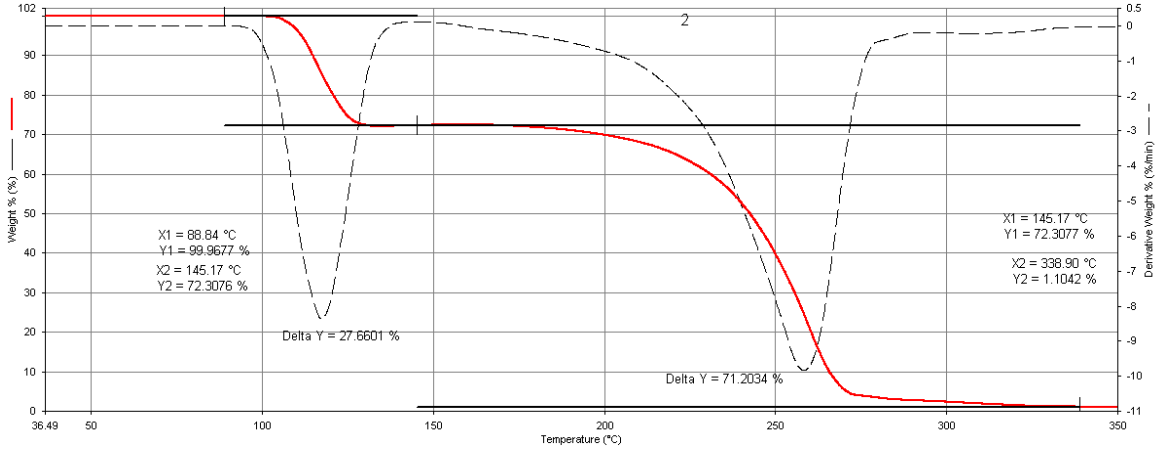

Figure S33 DSC measurement of the compound **2.**

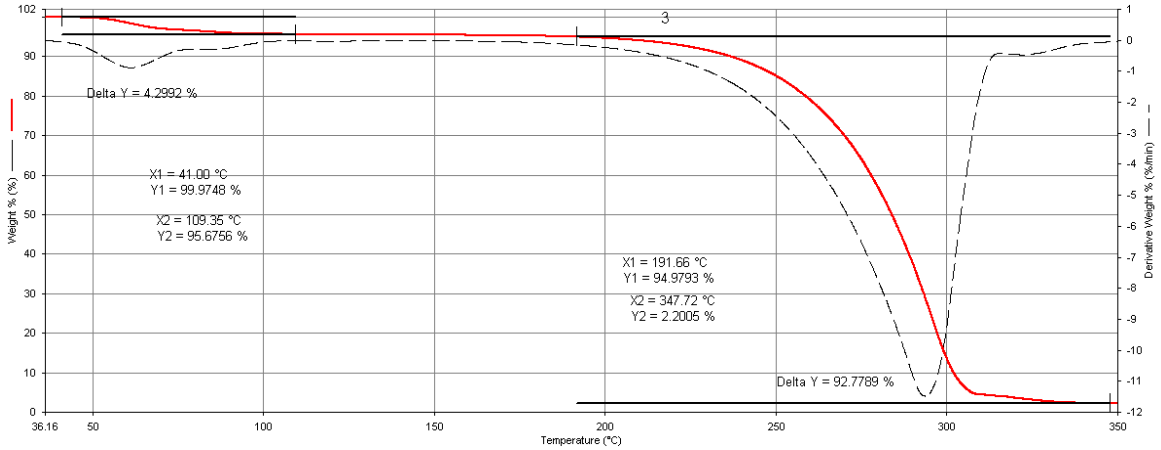

Figure S34 DSC measurement of the compound **3$_{solv}$.**

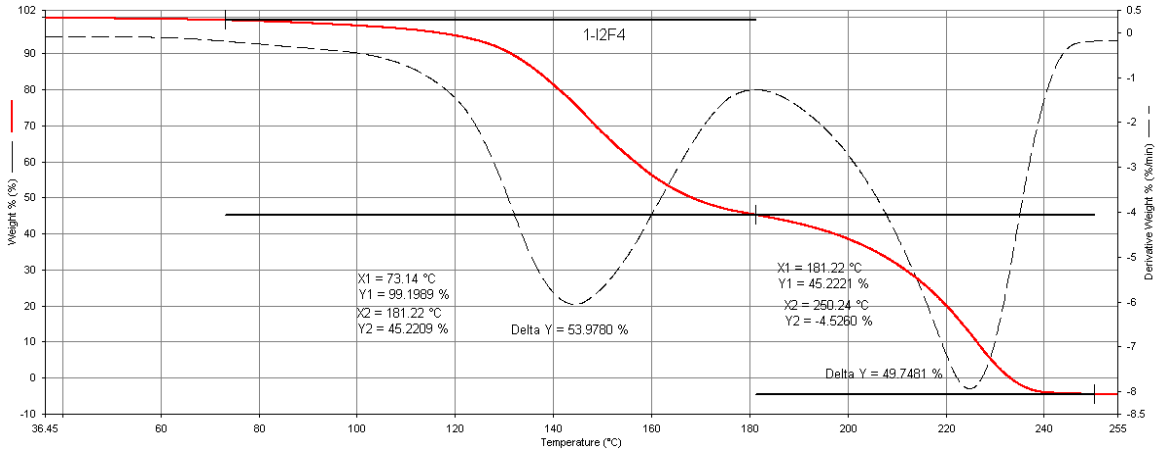

Figure S35 DSC measurement of the compound **1$_2$·I2F4.**

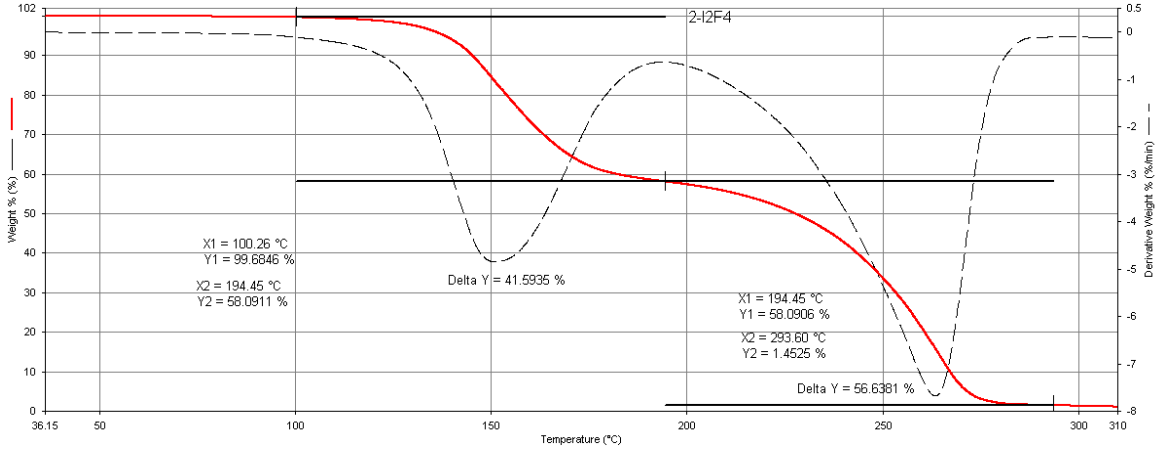

Figure S36 DSC measurement of the compound **2$_2$·I2F4**.

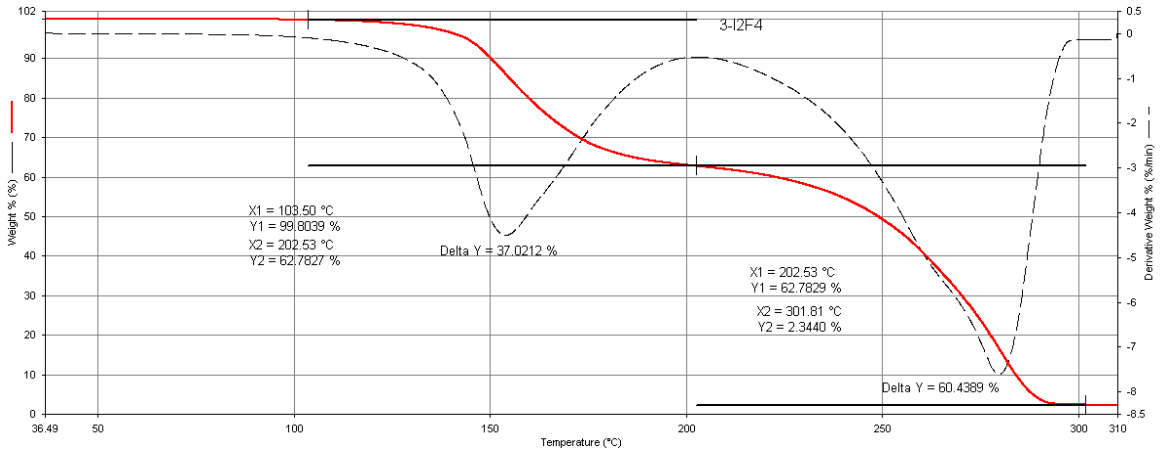

Figure S37 DSC measurement of the compound **3_2·I2F4.**

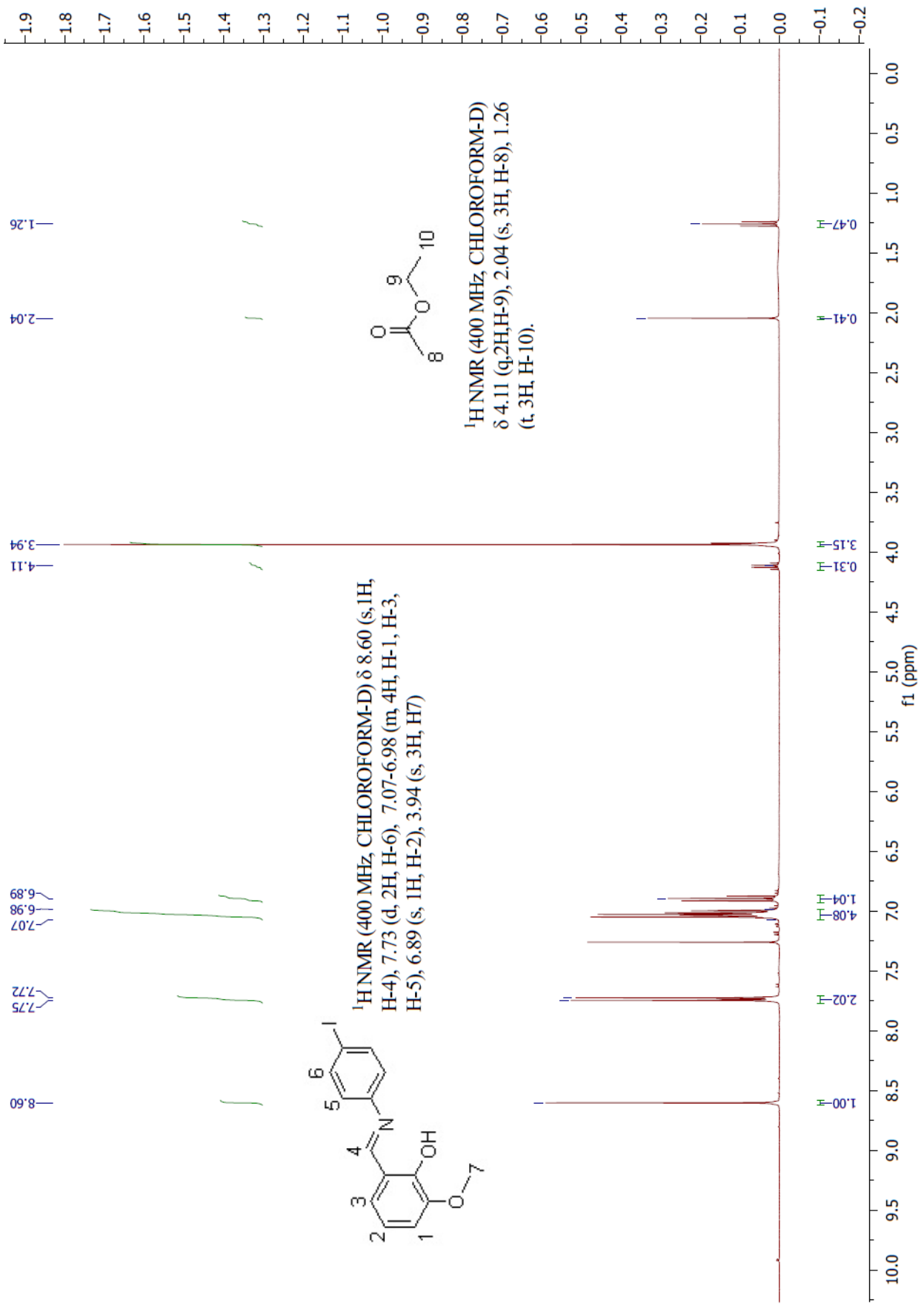

Figure S38 ^{1}H NMR spectrum of $\mathbf{3}_{\mathbf{solv}}$.